SYSTEMATIC COMPARISON OF HEAVY-ION FUSION BARRIERS CALCULATED WITHIN THE FRAMEWORK OF THE DOUBLE FOLDING MODEL USING TWO VERSIONS OF NUCLEON-NUCLEON INTERACTION

Igor Gontchar, Maria Chushnyakova
Omsk, Russia

Nucleus 2015

Experimental fusion excitation function

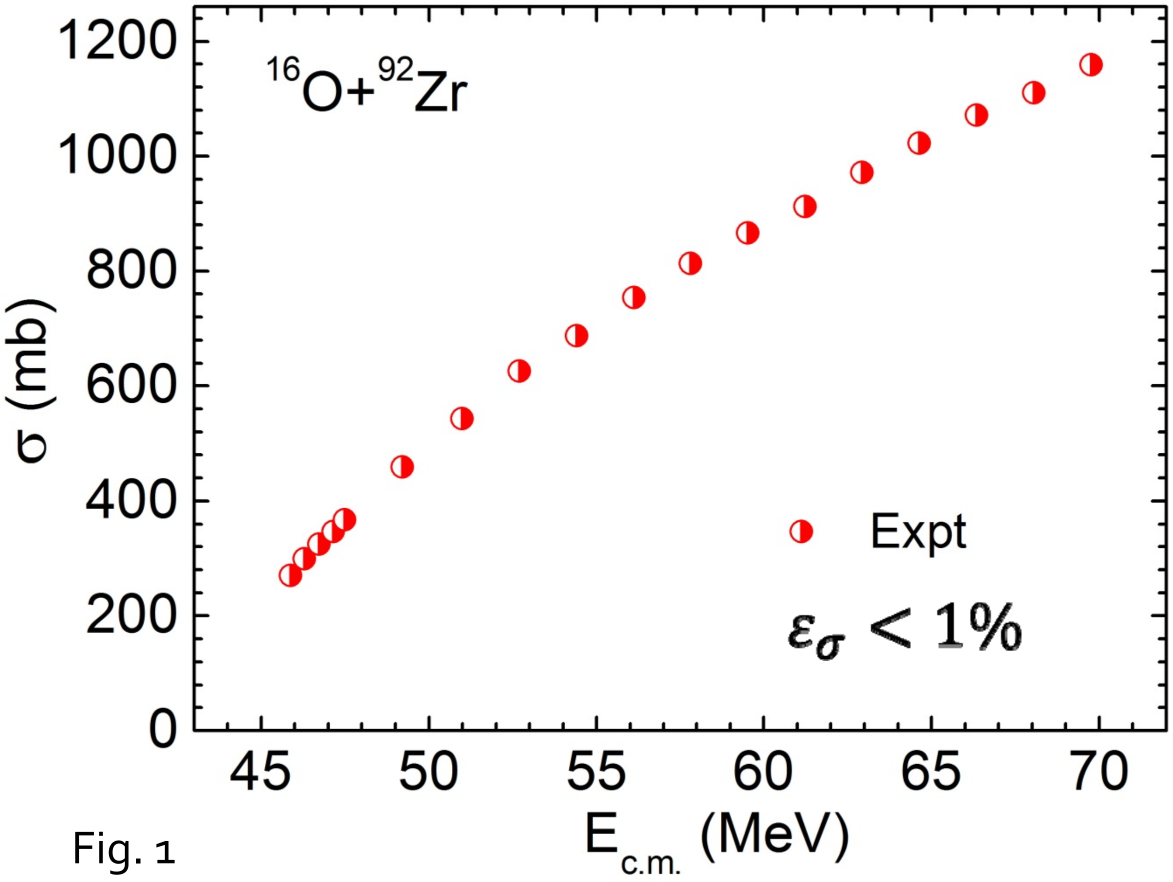

Fig. 1

[1] Newton et al., Phys. Rev. C 64, 064608 (2001)

Theoretical description

- **CCM**: Coupled channels model – reasonable for the subbarrier cross sections

- **BPM**: Single barrier penetration model – gives the upper limit of excitation function

- **TMSF**: Trajectory model with surface friction –
  accounts for the energy dissipation; moves down the excitation function

Double folding potentials with

- **M3Y** effective *NN* (nucleon-nucleon) interaction [2-4]

- **Migdal** effective *NN* interaction [5]

[2] Satchler, Love, Phys. Rep. 55, 183 (1979)
[3] Bertsch et al., Nucl. Phys. A 284 (1977) 399
[4] Anantaraman et al. Nucl. Phys. A 398 (1983) 269
[5] Migdal, Theory of Finite Fermi Systems and Applications to Atomic Nuclei (Interscience, New York, 1967)

Comparison of our fluctuation-dissipation model with the experiment for a single reaction

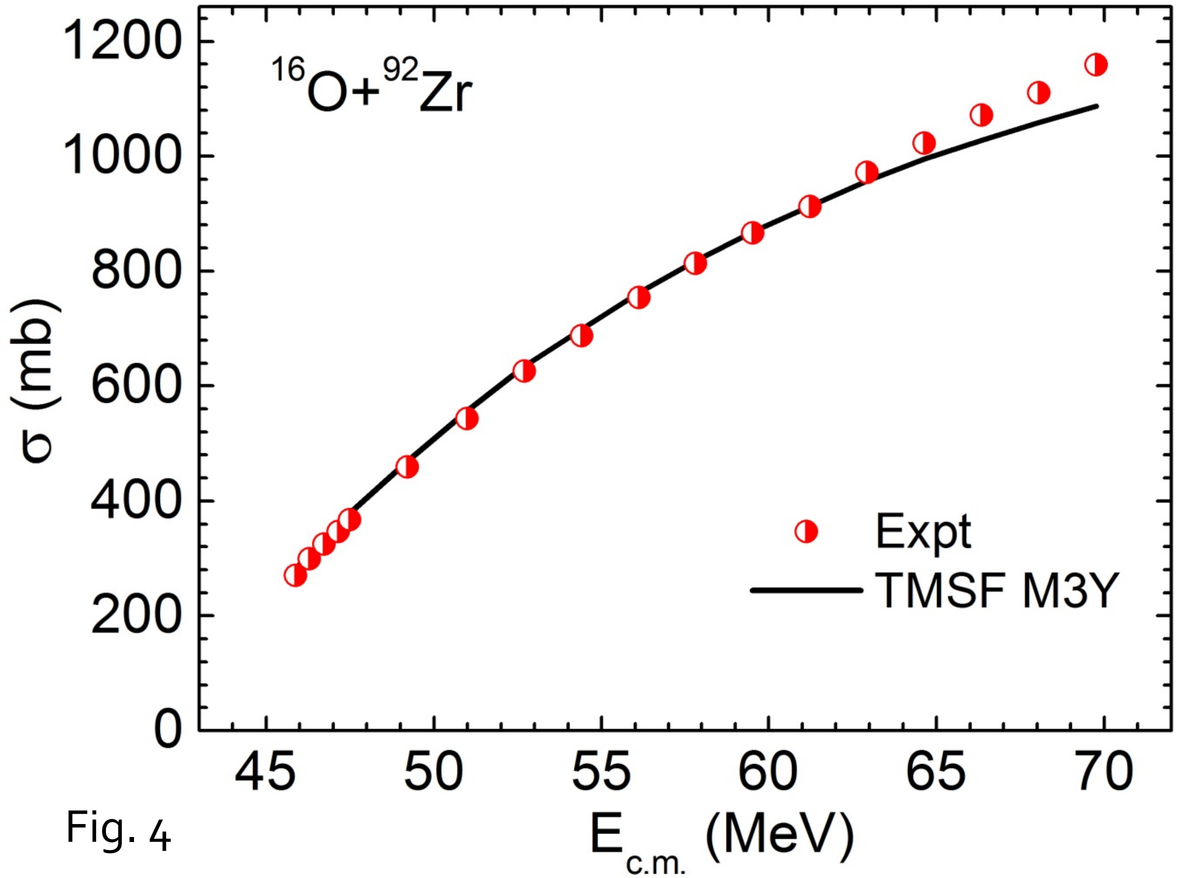

Fig. 4

[6] Chushnyakova, Bhattacharya, Gontchar, Phys. Rev. C 90, 017603 (2014)

M3Y vs experiment (91 points)

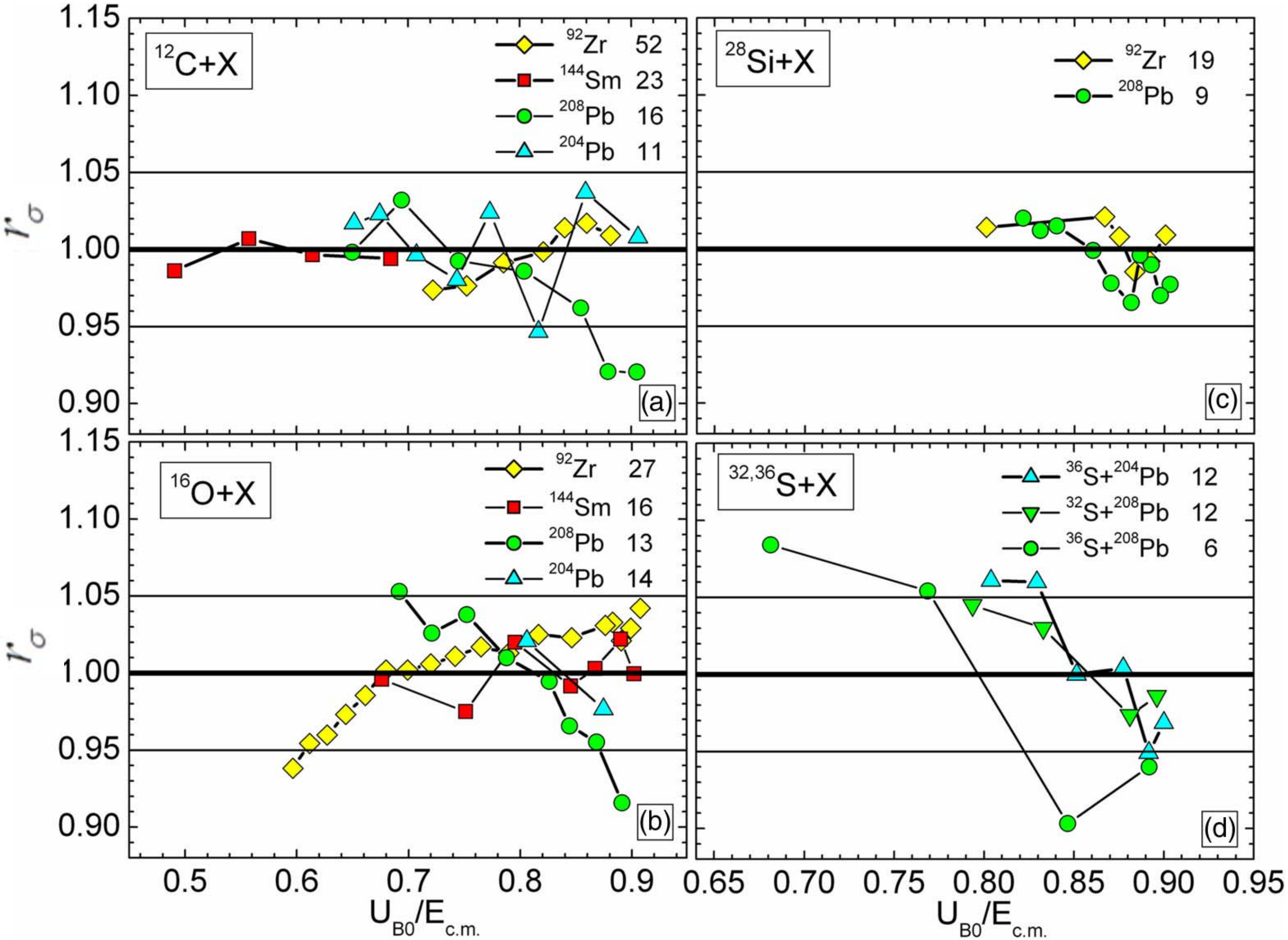

Fig. 5

$$r_\sigma = \sigma_{th} / \sigma_{\exp} \qquad (1)$$

M3Y vs experiment (91 points)

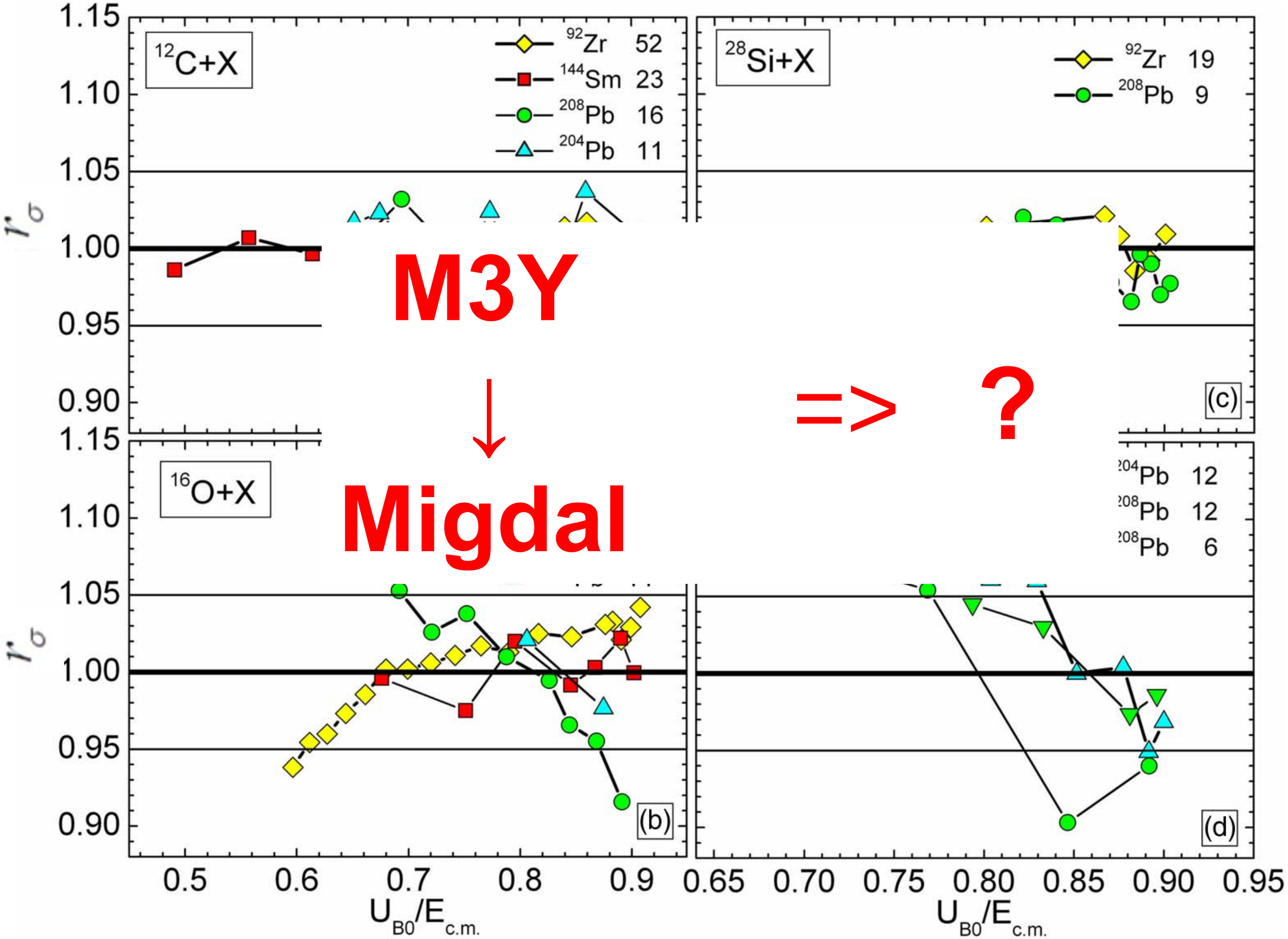

Fig. 5

$$r_\sigma = \sigma_{th} / \sigma_{\exp} \qquad (1)$$

Double-folding model with M3Y *NN* interaction:

$$U_n(R,E_P) = U_{nD}(R,E_P) + U_{nE}(R,E_P) \qquad (2)$$

$$U_{nD}(R,E_P) = g(E_P)\int d\vec{r}_P \int d\vec{r}_T\, \rho_{AP}(\vec{r}_P)\, F_{\rm v}(\rho_{FA})\, {\rm v}_D(s)\, \rho_{AT}(\vec{r}_T) \qquad (3)$$

Density Dependent M3Y

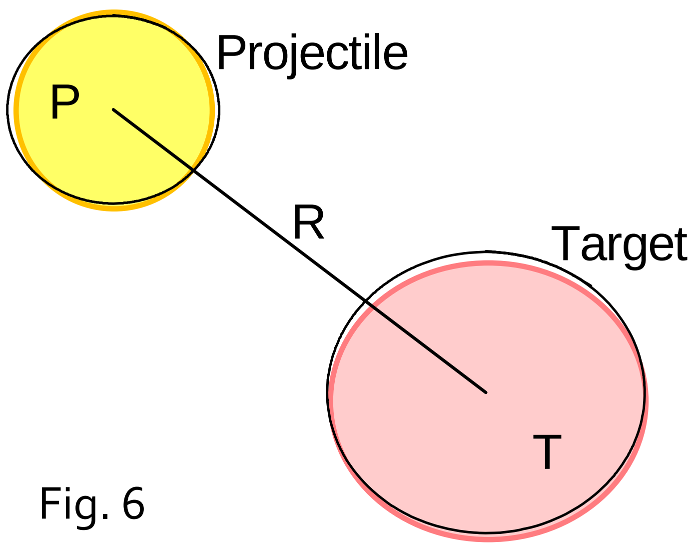

Fig. 6

$${\rm v}_D(s) = \sum_{i=1}^{3} G_{Di}[\exp(-s/r_{{\rm v}i})]/(s/r_{{\rm v}i}) \qquad (4)$$

[7] Khoa et al., Phys. Rev. C 56, 954 (1997)
[8] Gontchar, Chushnyakova, Comp. Phys. Comm. 181 (2010) 168–182

Double-folding model with Migdal forces:

The quote from
Zagrebaev et al., Phys. Elem. Part. At. Nucl. 38, 892 (2007).

$$v_{NN}^{(N)}(\mathbf{r}_1,\mathbf{r}_2) =$$

$$= C\left[F_{\rm ex} + (F_{\rm in} - F_{\rm ex})\frac{\rho_1(\mathbf{r}_1)+\rho_2(\mathbf{r}_2)}{\rho_{00}}\right]\delta(\mathbf{r}_{12}) = v_{\rm eff}(\mathbf{r}_1,\mathbf{r}_2)\delta(\mathbf{r}_{12}), \quad (17)$$

где

$$F_{\rm ex(in)} = f_{\rm ex(in)} \pm f'_{\rm ex(in)}. \quad (18)$$

Здесь знак «плюс» соответствует взаимодействию одинаковых частиц (протон–протон или нейтрон–нейтрон), а «минус» — разных (протон–ней-

$$C = 300 \ \text{МэВ} \cdot \text{Фм}^3$$

$$f_{\rm in} = 0{,}09;\ f_{\rm ex} = -2{,}59;\ f'_{\rm in} = 0{,}42;\ f'_{\rm ex} = 0{,}54.$$

Double-folding model with Migdal forces:

$$U_{nMIG}(R) = \int d\vec{r_P} \int d\vec{r_T} \Big[\rho_{Pn}(\vec{r_P}) v_{nn}(s) \rho_{Tn}(\vec{r_T}) + \rho_{Pp}(\vec{r_P}) v_{pp}(s) \rho_{Tp}(\vec{r_T}) + \\ + \rho_{Pn}(\vec{r_P}) v_{np}(s) \rho_{Tp}(\vec{r_T}) + \rho_{Pp}(\vec{r_P}) v_{pn}(s) \rho_{Tn}(\vec{r_T})\Big] \qquad (5)$$

$$v_{nn}(\vec{r_P},\vec{r_T}) = \left[a + 2(g-a)\frac{\rho_{Pn}(\vec{r_P}) + \rho_{Tn}(\vec{r_T})}{\rho_{Pn}(0) + \rho_{Tn}(0)}\right]\delta(\vec{s})$$

$$v_{pp}(\vec{r_P},\vec{r_T}) = \left[a + 2(g-a)\frac{\rho_{Pp}(\vec{r_P}) + \rho_{Tp}(\vec{r_T})}{\rho_{Pp}(0) + \rho_{Tp}(0)}\right]\delta(\vec{s}) \qquad (6)$$

$$v_{np}(\vec{r_P},\vec{r_T}) = \left[\varphi + 2(\gamma-\varphi)\frac{\rho_{Pn}(\vec{r_P}) + \rho_{Tp}(\vec{r_T})}{\rho_{Pn}(0) + \rho_{Tp}(0)}\right]\delta(\vec{s})$$

$$v_{pn}(\vec{r_P},\vec{r_T}) = \left[\varphi + 2(\gamma-\varphi)\frac{\rho_{Pp}(\vec{r_P}) + \rho_{Tn}(\vec{r_T})}{\rho_{Pp}(0) + \rho_{Tn}(0)}\right]\delta(\vec{s})$$

[5] Migdal, Theory of Finite Fermi Systems and Applications to Atomic Nuclei (Interscience, New York, 1967)
[9] Zagrebaev et al., Phys. Elem. Part. At. Nucl. 38, 892 (2007).

Two versions of the *NN* potential

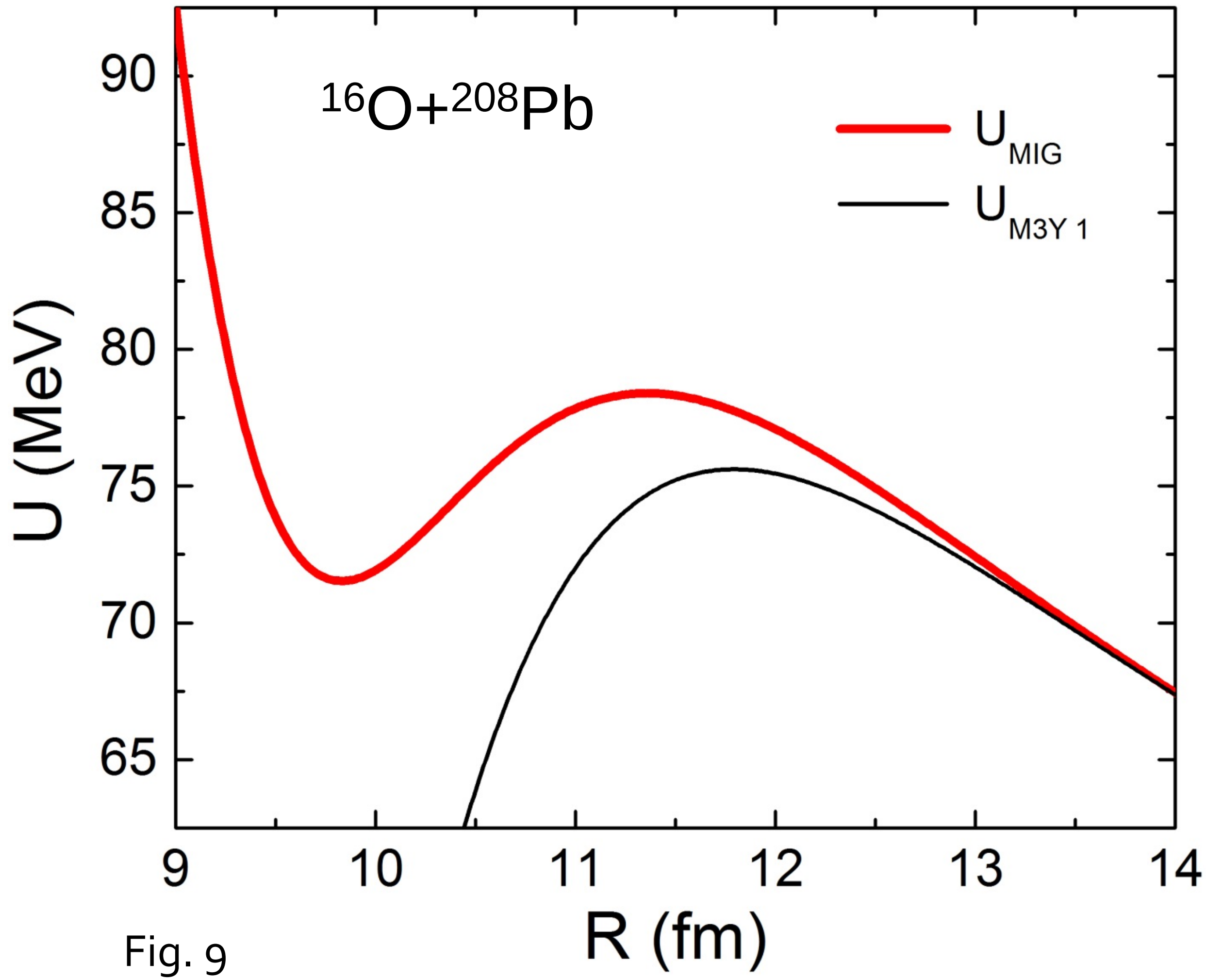

Fig. 9

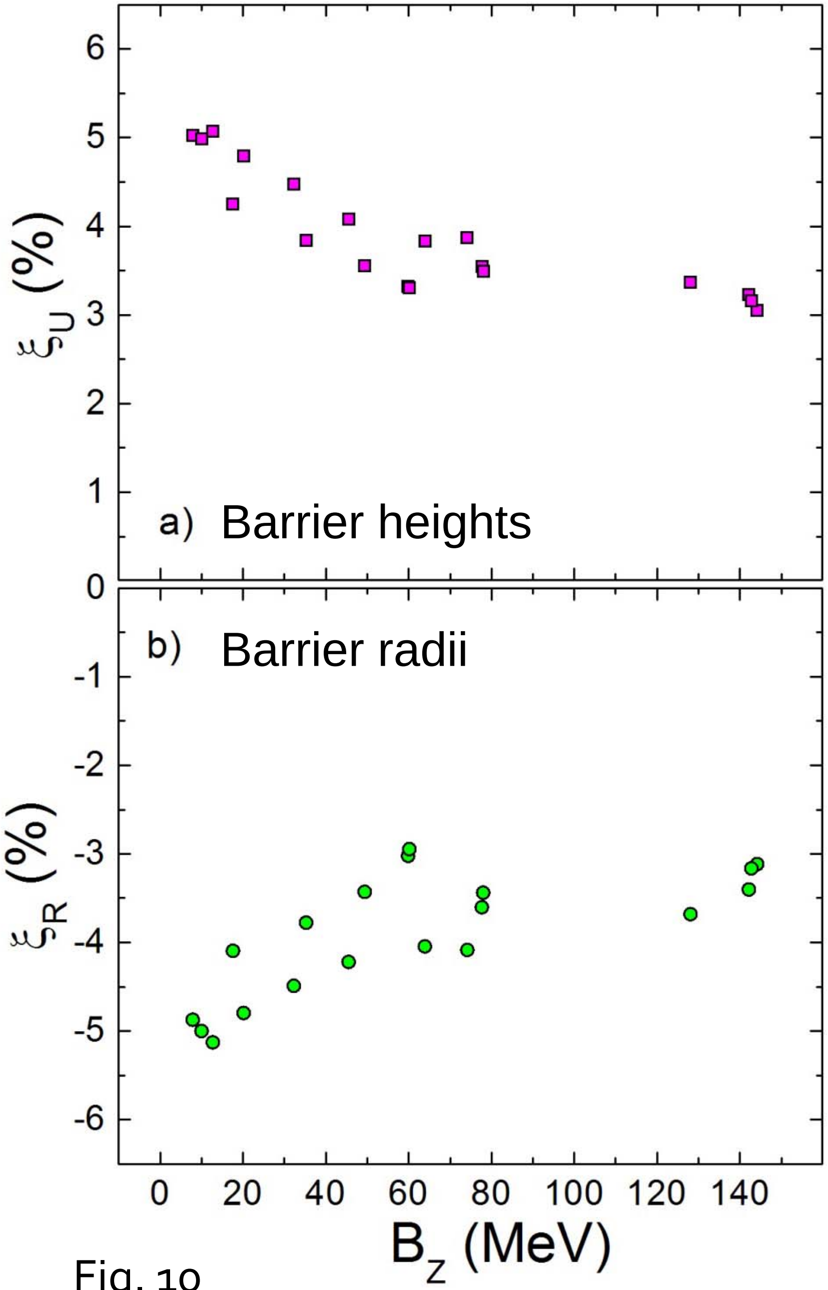

Fig. 10

M3Y vs Migdal:

Systematic comparison of the barriers

$$\xi_U = \frac{U_{B0Mig} - U_{B0M3Y}}{U_{B0Mig}} \quad (7)$$

$$B_Z = Z_P Z_T / \left(A_P^{1/3} + A_T^{1/3} \right) \quad (8)$$

Comparison of BPM cross sections with the experimental ones for a single reaction

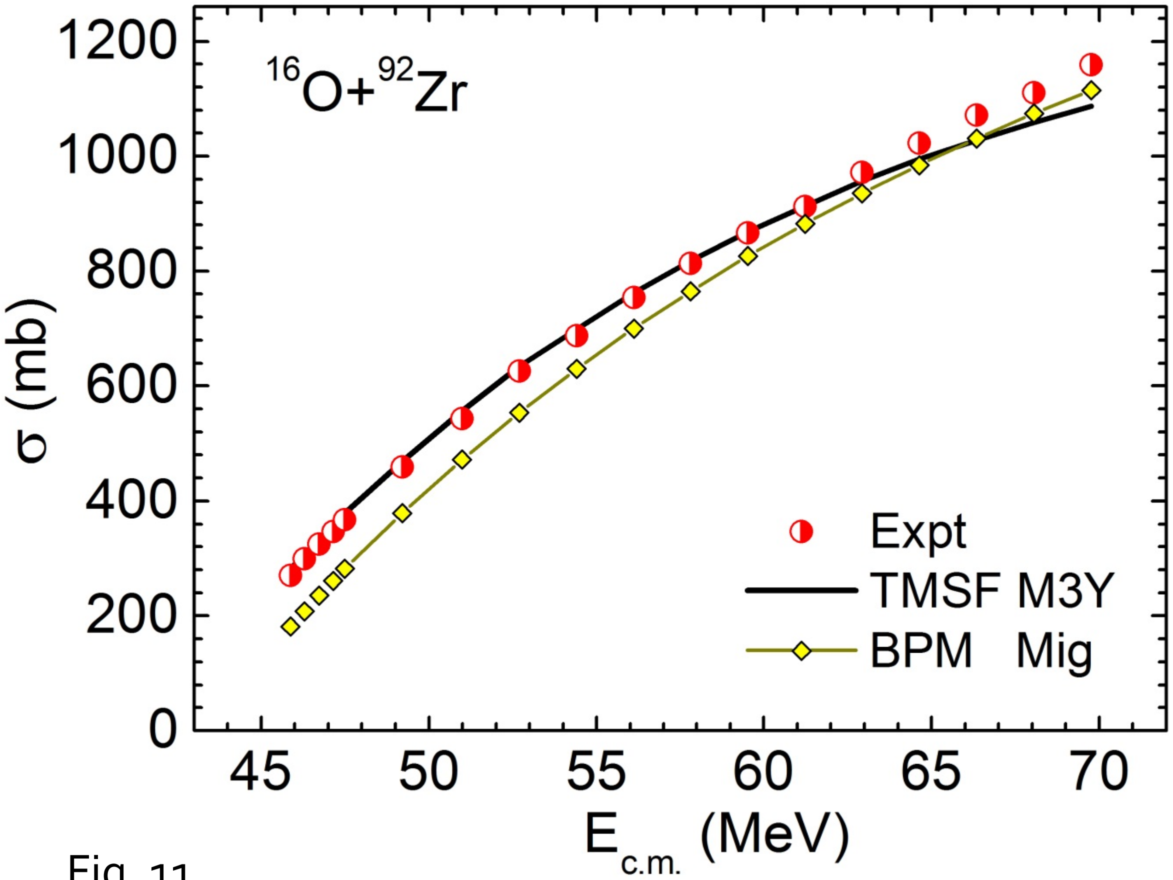

Fig. 11

[1] J. O. Newton et al., Phys. Rev. C 64, 064608 (2001)

Comparison of BPM cross sections with the experimental ones for a single reaction

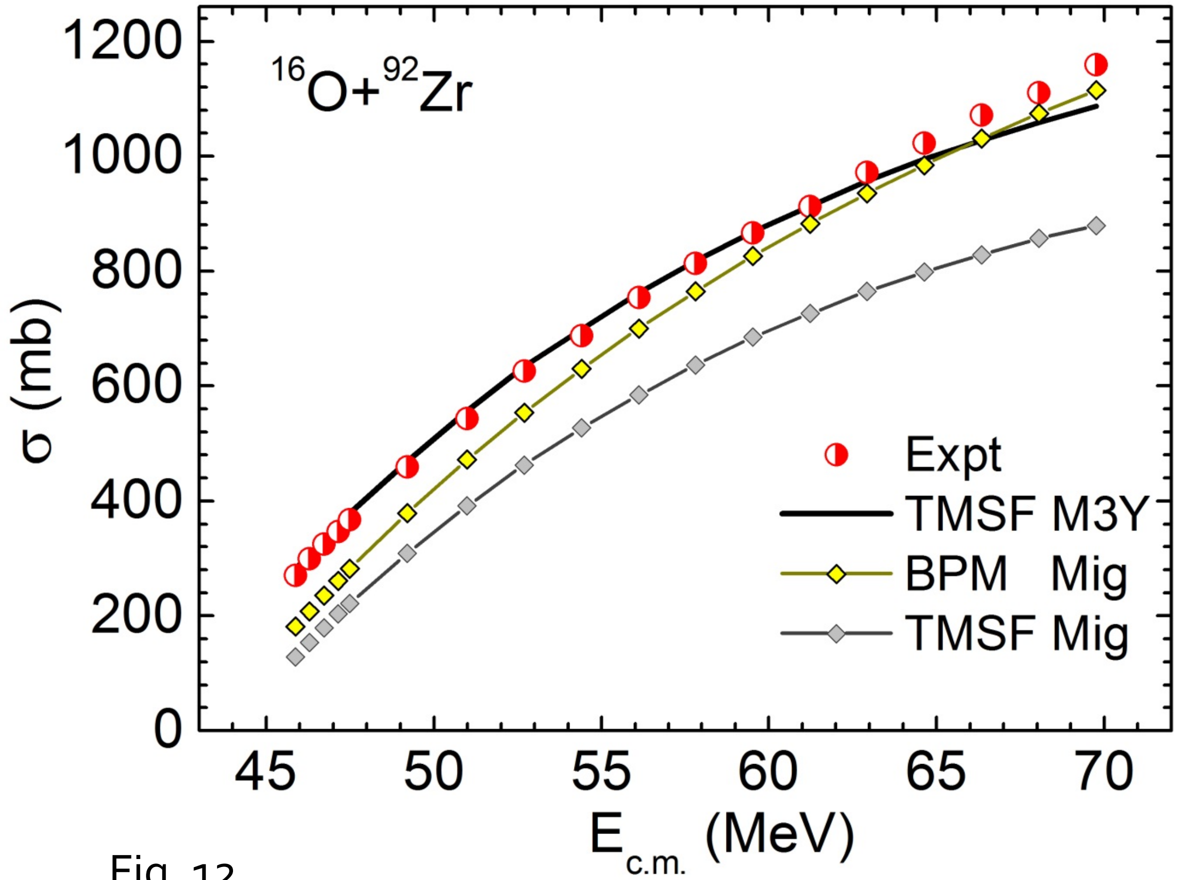

Fig. 12

[1] J. O. Newton et al., Phys. Rev. C 64, 064608 (2001)

Migdal vs experiment (91 points)

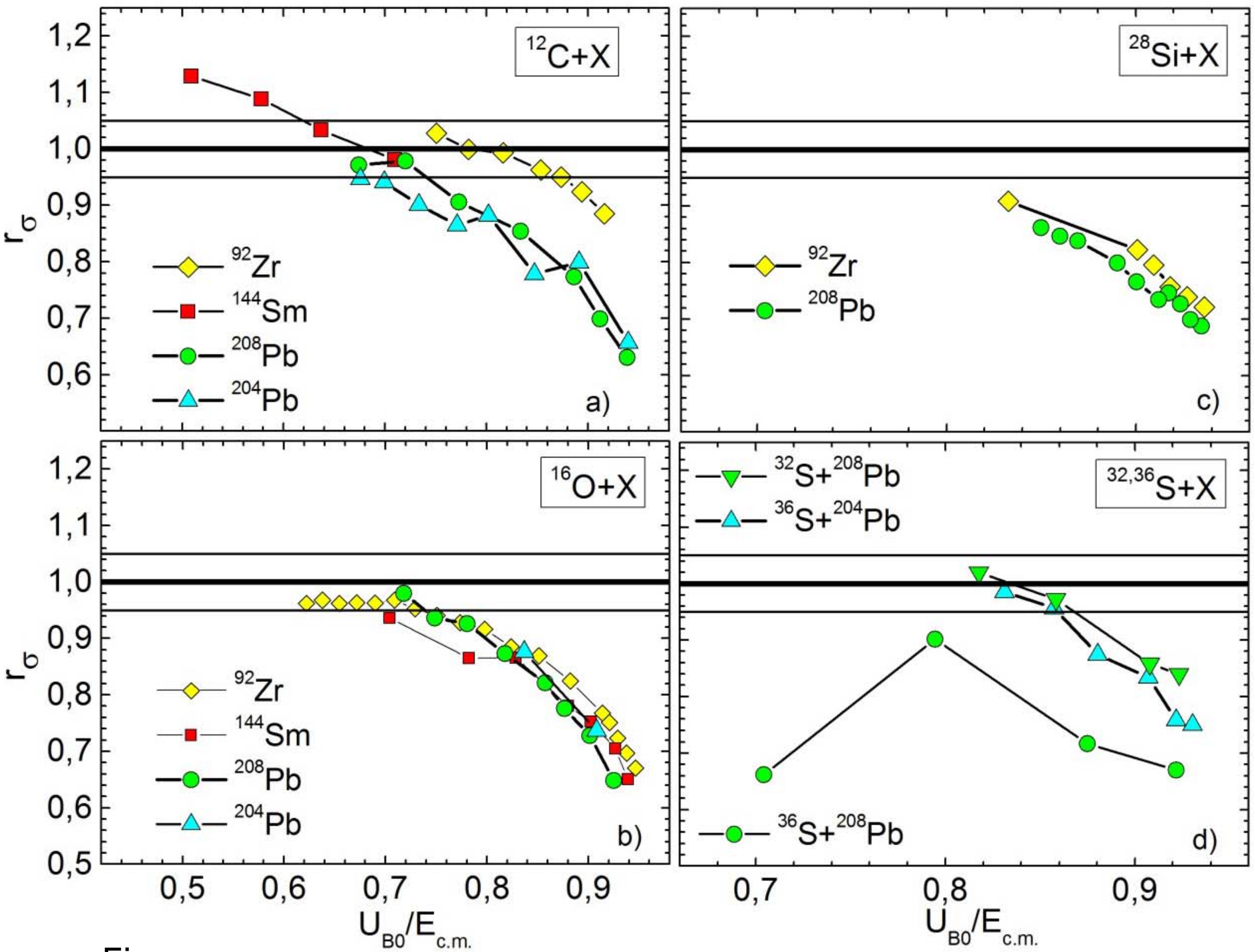

Fig. 13

$$r_\sigma = \sigma_{th} / \sigma_{\exp} \qquad (1)$$

Conclusions

The comparison made for 19 reactions with spherical nuclei revealed that the Migdal barriers are always higher by several percent than the M3Y barriers.

This results in rather low fusion cross sections calculated with the Migdal forces:

most of the calculated cross sections significantly (up to 40%) underestimates the experimental values.

Using the Migdal nucleon-nucleon interaction with the constants from Ref. [5] for describing fusion (capture) cross sections is questionable.

[5] A. B. Migdal, Theory of Finite Fermi Systems and Applications to Atomic Nuclei (Interscience, New York, 1967).

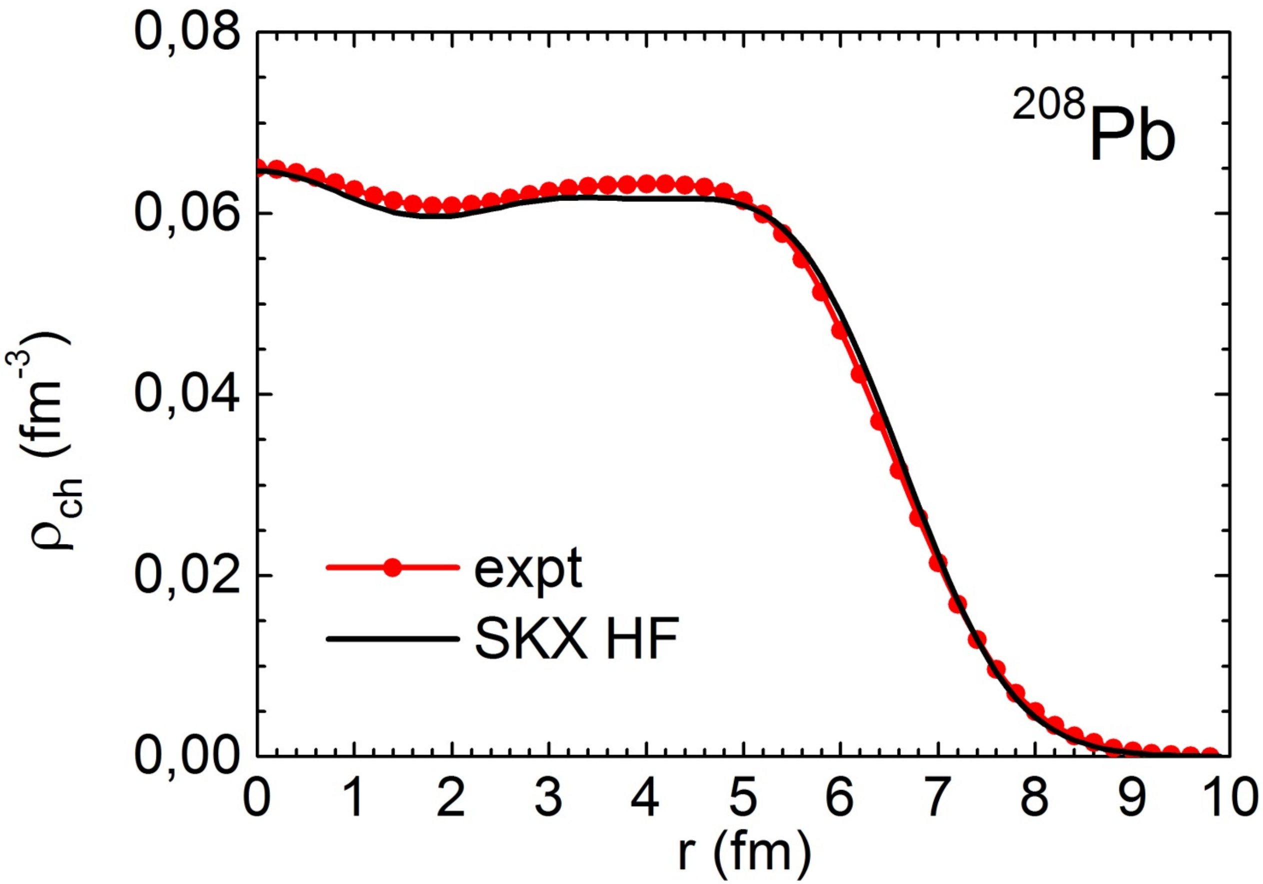

Fig. 030. Comparison of the experimental charge density [10] with the calculated one within the Hartree-Fock approach with the SKX coefficient set

[10] H. de Vries et al., At. Data Nucl. Data Tables 36, 495 (1987)

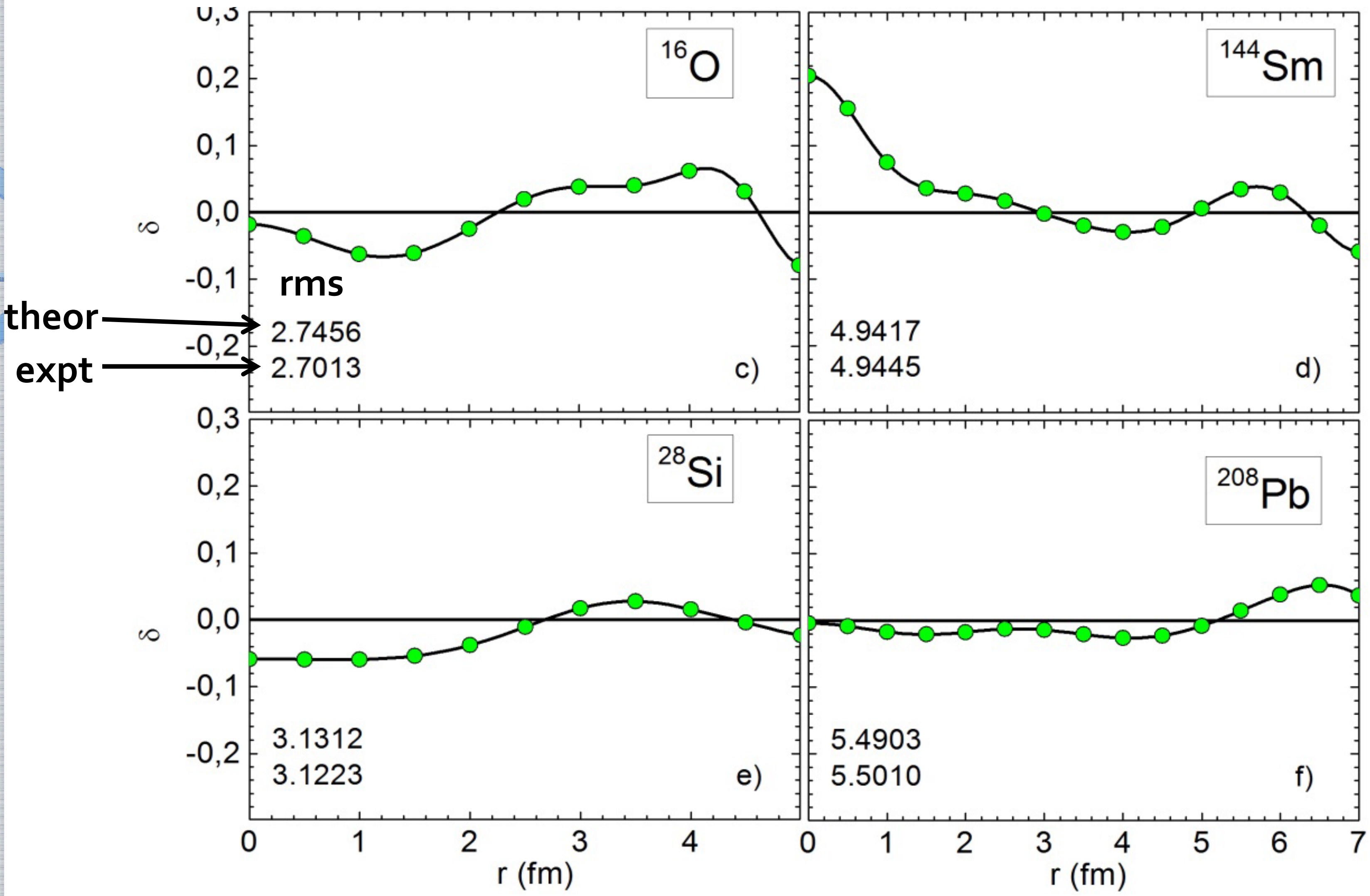

$$\delta = 2\left(\rho_{\text{ch th}} - \rho_{\text{ch exp}}\right) / \left(\rho_{\text{ch th}} + \rho_{\text{ch exp}}\right) \qquad (20)$$

The ratio of the calculated rms charge radius $R_{q\ th}$ to the experimental one $R_{q\ exp}$ [10].

Nucleus	^{12}C	^{16}O	^{28}Si	^{32}S	^{36}S	^{92}Zr	^{144}Sm	^{204}Pb	^{208}Pb
$R_{q\ th} / R_{q\ exp}$	1.0199	1.0164	1.0029	0.9987	1.0006	0.9952	0.9994	0.9985	0.9981

[10] H. de Vries et al., At. Data Nucl. Data Tables 36, 495 (1987)

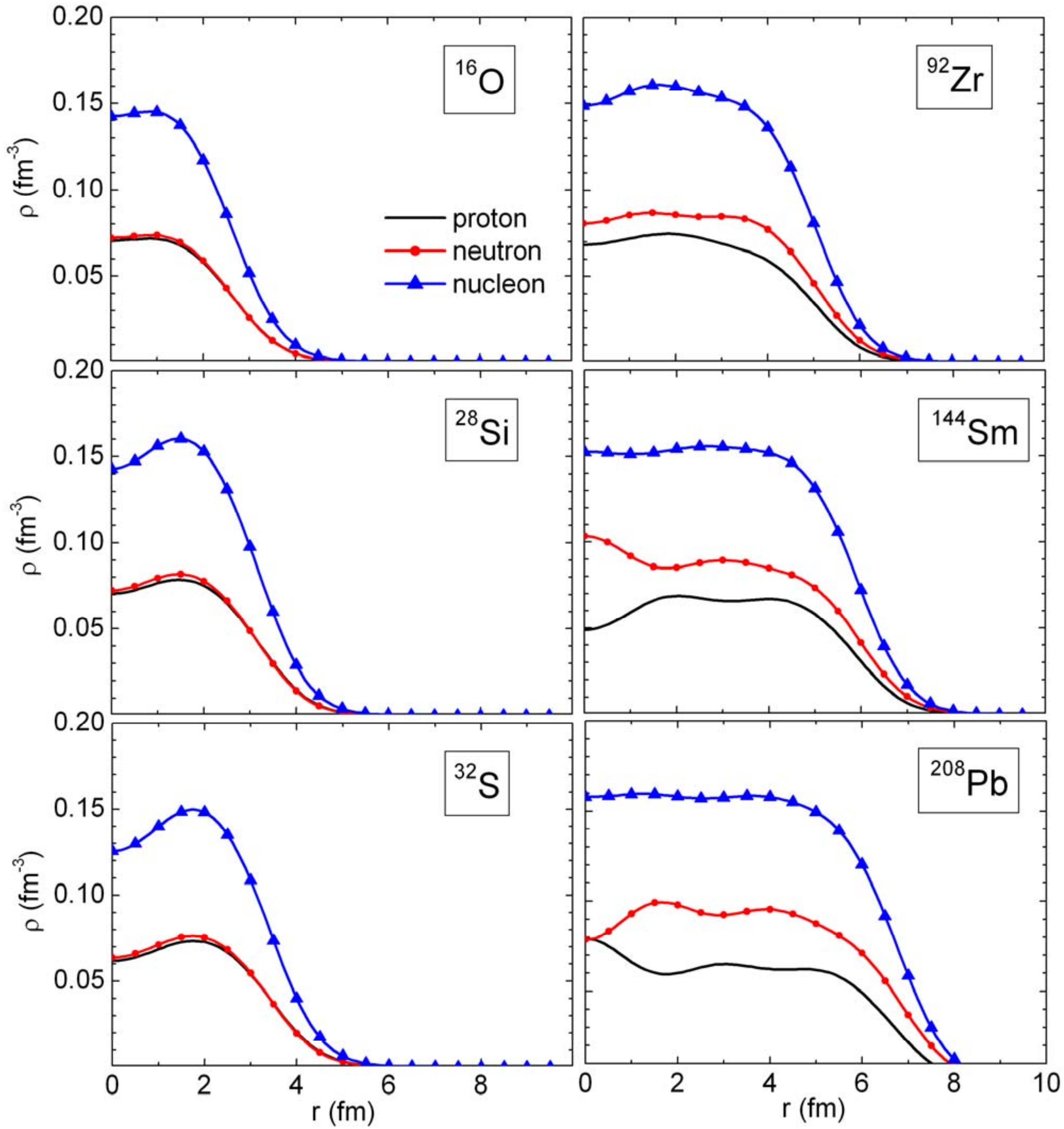

^{16}O
^{92}Zr
^{28}Si
^{144}Sm
^{32}S
^{208}Pb
proton
neutron
nucleon
ρ (fm^{-3})
r (fm)
0.20
0.15
0.10
0.05
0
2
4
6
8
10

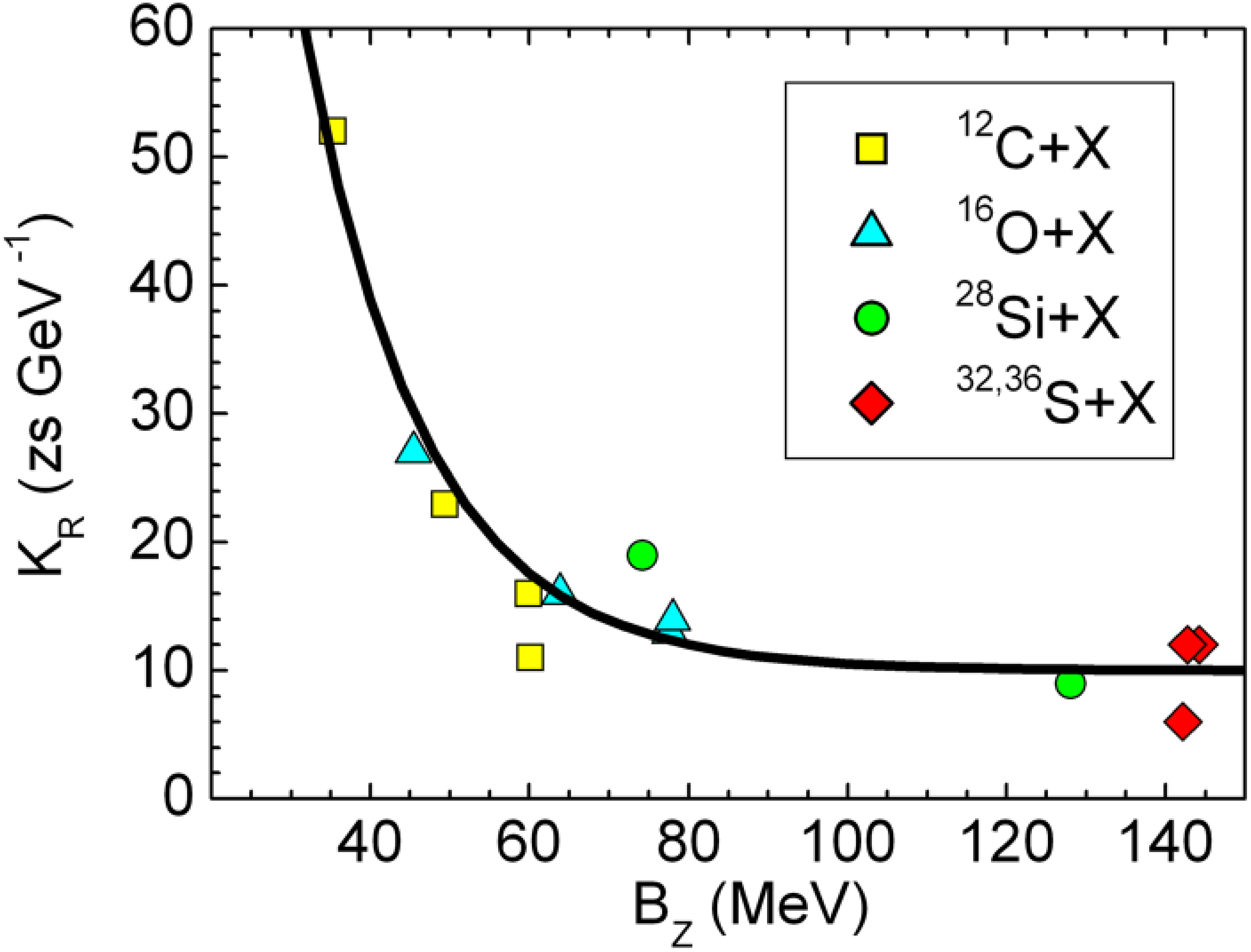

K_R (zs GeV^{-1})
B_Z (MeV)
^{12}C+X
^{16}O+X
^{28}Si+X
^{32,36}S+X
0
10
20
30
40
50
60
40
60
80
100
120
140

Reactions	Expt. data Refs.
$^{12}C+^{92}Zr$, $^{16}O+^{92}Zr$, $^{28}Si+^{92}Zr$	[1] Newton et al., Phys. Rev. C 64, 064608 (2001)
$^{12}C+^{144}Sm$	[11] Kossakowski et al., Phys.Rev. C 32, 1612 (1985)
$^{12}C+^{208}Pb$	[12] Mukherjee, Hinde et al., Phys. Rev. C 75, 044608 (2007)
$^{12}C+^{204}Pb$	[13] Berriman, Hinde et al, Nature (London) 413, 144 (2001)
$^{16}O+^{144}Sm$	[14] Leigh, Dasgupta et al., Phys. Rev. C 52, 3151 (1995)
$^{16}O+^{208}Pb$	[15] Morton, Berriman et al., Phys. Rev. C 60, 044608 (1999)
$^{16}O+^{204}Pb$	[16] Dasgupta et al, Phys. Rev. Lett. 99, 192701 (2007)
$^{28}Si+^{208}Pb$, $^{32}S+^{208}Pb$	[17] Hinde et al., Nucl. Phys. A 592, 271 (1995).
$^{36}S+ {}^{208}Pb$	[18] Yanez et al., Phys. Rev. C 82, 054615 (2010)
$^{36}S+ {}^{204}Pb$	[19] Hinde et al., Phys. Rev. C 75, 054603 (2007)

Таблица 3

Нулевые гармоники амплитуды $\mathcal{F}$ *)

	[52] Варианты I	[52] Варианты II	[108], [57]	[109]	[111]
1	2		3	4	5
f_{in}	—0,09	+0,09	0,25	~0,5	—
f_{ex}	—2,23	—2,59	—2,5	~—2,7	—
f'_{in}	0,89	0,42	0,95	~0,93	—
f'_{ex}	0,06	0,54	$= f'_{in}$	$= f'_{in}$	—
g	0,7	0,7	~0,5	—	0,7
g'	0,83	0,83	1,0	—	0,75 или 0,9

*) Пересчитанные на $C_0 = 300$ МэВ·ферми^3.

Fusion (capture) cross section

$$\sigma = \frac{\pi\hbar^2}{2m_R E_{c.m.}} \sum_{L=0}^{L_{\max}} (2L+1) T_L \qquad (1)$$

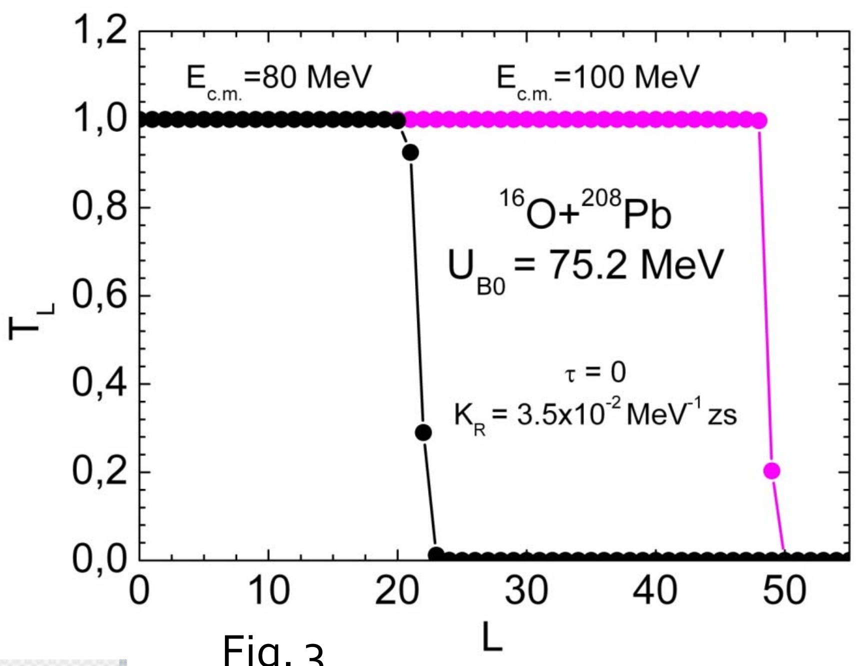

Fig. 3

Single Barrier Penetration Model

$$T_L = \frac{1}{1+\exp\left[2\pi\left(U_{BL} - E_{c.m.}\right)/\left(\hbar\omega_{BL}\right)\right]} \qquad (2)$$

Woods-Saxon profile:

$$U_n(R) = V_{WS}\left\{1 + \exp\left(\frac{R - r_{WS}\left(A_P^{1/3} + A_T^{1/3}\right)}{a_{WS}}\right)\right\}^{-1} \quad (3)$$

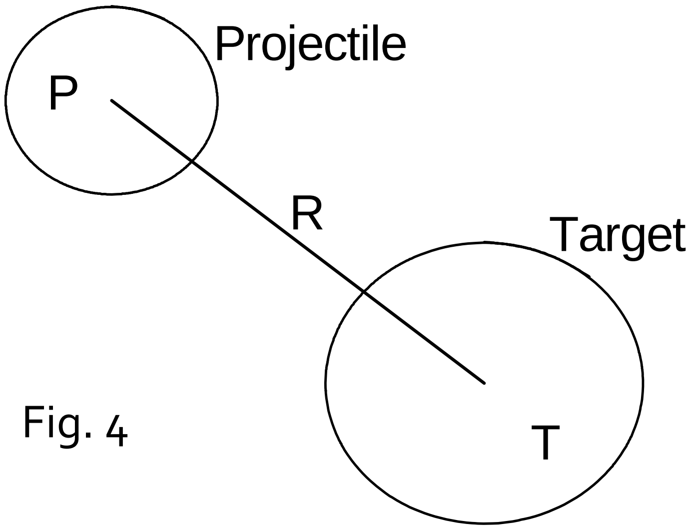

Fig. 4

Classical Trajectory Model with the Surface Friction (TMSF)

$$dp_q = \left(F_U + F_{cen} + \Phi_{Dq}\right)dt + \xi\chi\sqrt{2D_q dt} \quad (5) \qquad dq = \frac{p_q}{m_q}dt \quad (6)$$

$$F_U = -\frac{dU_{tot}}{dq} \quad (7) \qquad F_{cen} = \frac{\hbar^2 L^2}{m_q q^3} \quad (8)$$

$$\Phi_{Dq} = -\int_0^t F_{Dq}(s)\Gamma(t-s)ds \quad (9) \qquad F_{Dq} = -\frac{p_q}{m_q}K_R\left(\frac{dU_n}{dq}\right)^2 \quad (10)$$

$$\Gamma(t-s) = \frac{1}{\tau}\exp\left(-\frac{|t-s|}{\tau}\right) \quad (11) \qquad D_q = \theta K_R\left(\frac{dU_n}{dq}\right)^2 \quad (12)$$

$$<\xi(t)>= 0 \quad (13) \qquad <\xi(t_1)\xi(t_2)>= \Gamma(t_1 - t_2) \quad (14)$$

[2] D.H.E. Gross, H. Kalinowski, Phys. Rep. 45 (1978) 175

[3] P. Fröbrich, Phys. Rep. 116 (1984) 337

Fusion (capture) cross section

$$\sigma = \frac{\pi\hbar^2}{2m_R E_{c.m.}} \sum_{L=0}^{L_{\max}} (2L+1) T_L \qquad (1)$$

TMSF

$$T_L = \frac{N_{cap\,L}}{N_{tot}} \qquad (15)$$

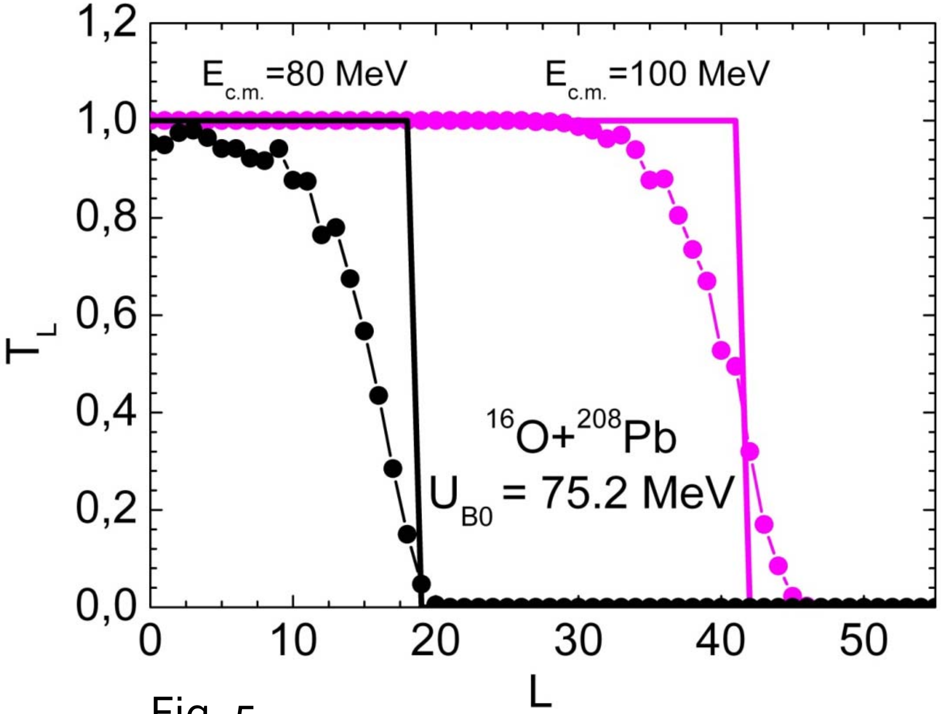

Fig. 5

Two versions of the *NN* potential

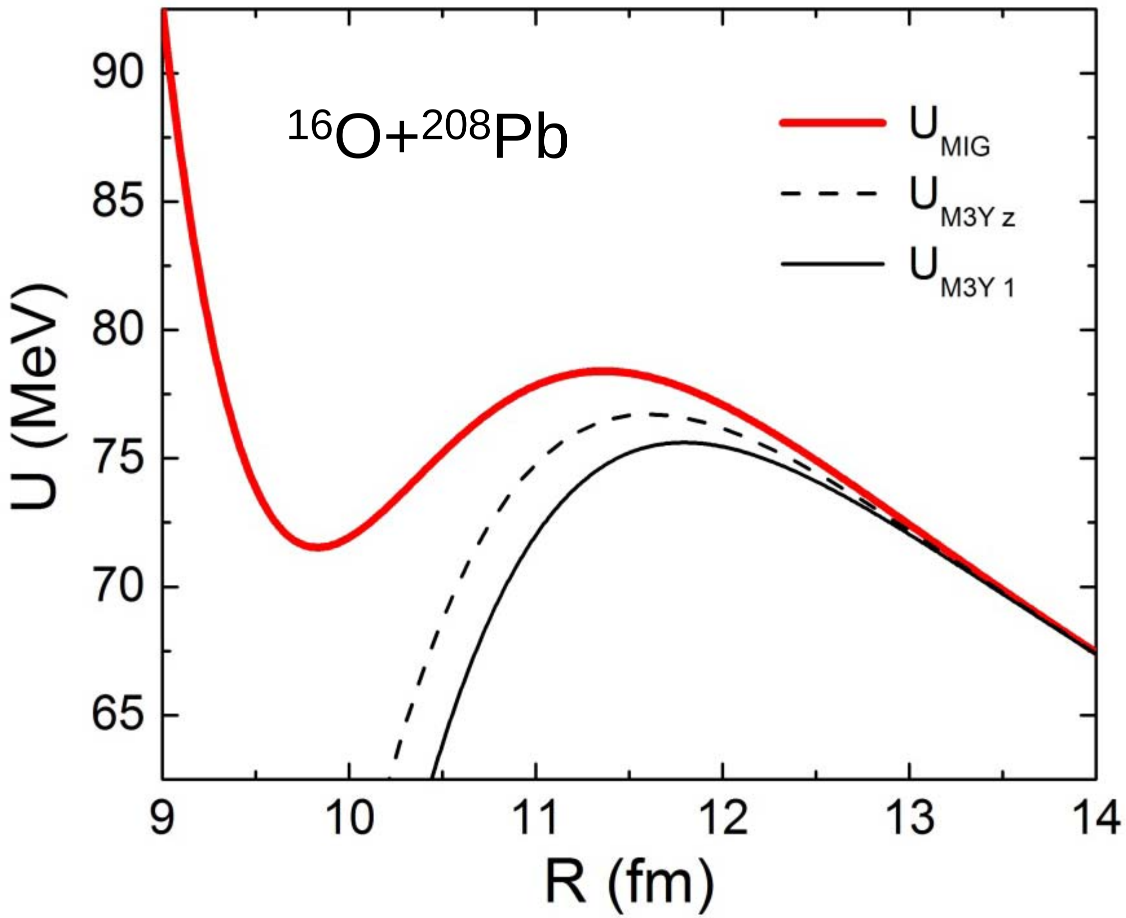

M3Y vs Migdal *NN* forces

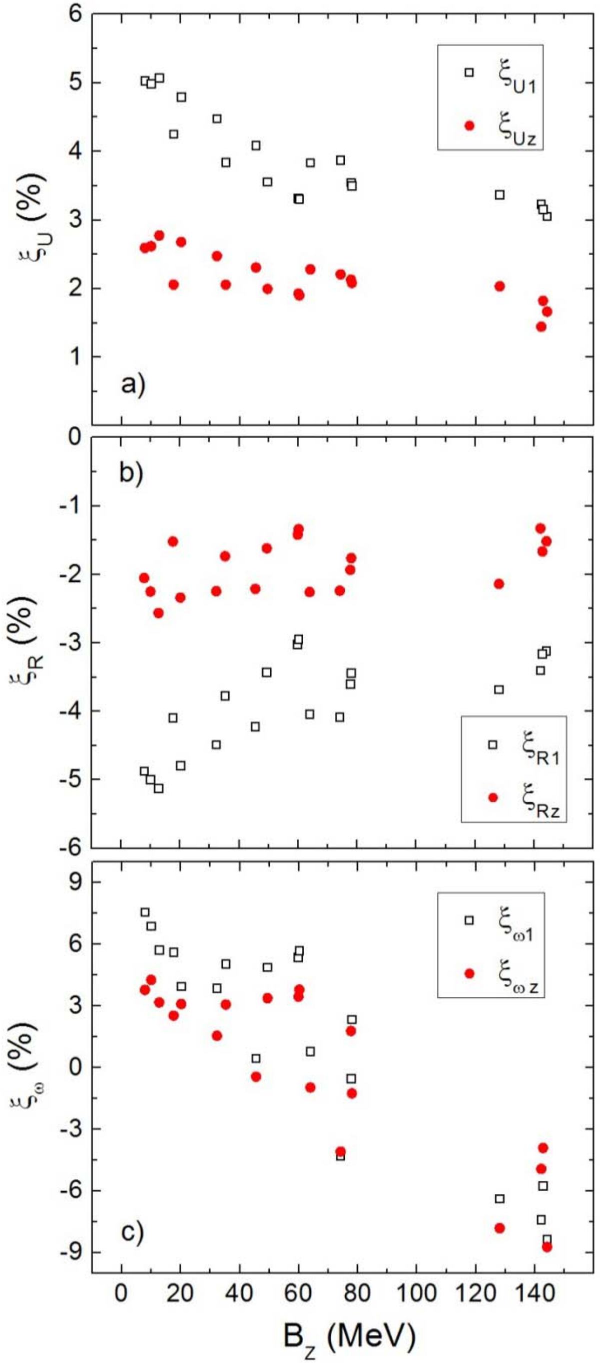

Systematic comparison of the fusion barrier parameters:

a) height

b) radius

c) curvature

Classical Trajectory Model with the Surface Friction (TMSF)

$$dp_q = \left(F_U + F_{cen} + \Phi_{Dq}\right)dt + \xi\chi\sqrt{2D_q dt} \quad (5) \qquad dq = \frac{p_q}{m_q}dt \quad (6)$$

$$dL = F_{D\varphi}dt + b\chi\sqrt{2D_\varphi dt} \quad (20) \qquad d\varphi = \frac{\hbar L}{m_q}dt \quad (21)$$

$$F_{D\varphi} = -\frac{\left(L - L_s\right)}{m_q}K_\varphi\left(\frac{dU_n}{dq}\right)^2 \quad (22) \qquad D_\varphi = \theta K_\varphi\left(\frac{dU_n}{dq}\right)^2 \quad (23)$$

[2] D.H.E. Gross, H. Kalinowski, Phys. Rep. 45 (1978) 175

[3] P. Fröbrich, Phys. Rep. 116 (1984) 337

Parameters of the matter distribution

$\langle R_{ch} \rangle$ [9] I. Angeli, At. Dat. Nucl. Dat. Tables 87 (2004) 185

$a_{ch} \approx \text{arbitrary}$

$$R_{0ch} = \sqrt{\frac{3}{5}\langle R_{ch} \rangle^2 - \frac{7\pi^2 a_{ch}^2}{5}} \quad (20)$$

$$R_{0ch} = R_{0A} \quad (22)$$

$$a_A^2 = a_{ch}^2 - \frac{5}{7\pi^2}\left(< r_{ch\,p}^2 > - < r_{ch\,n}^2 > \frac{N}{Z} \right) \quad (23)$$

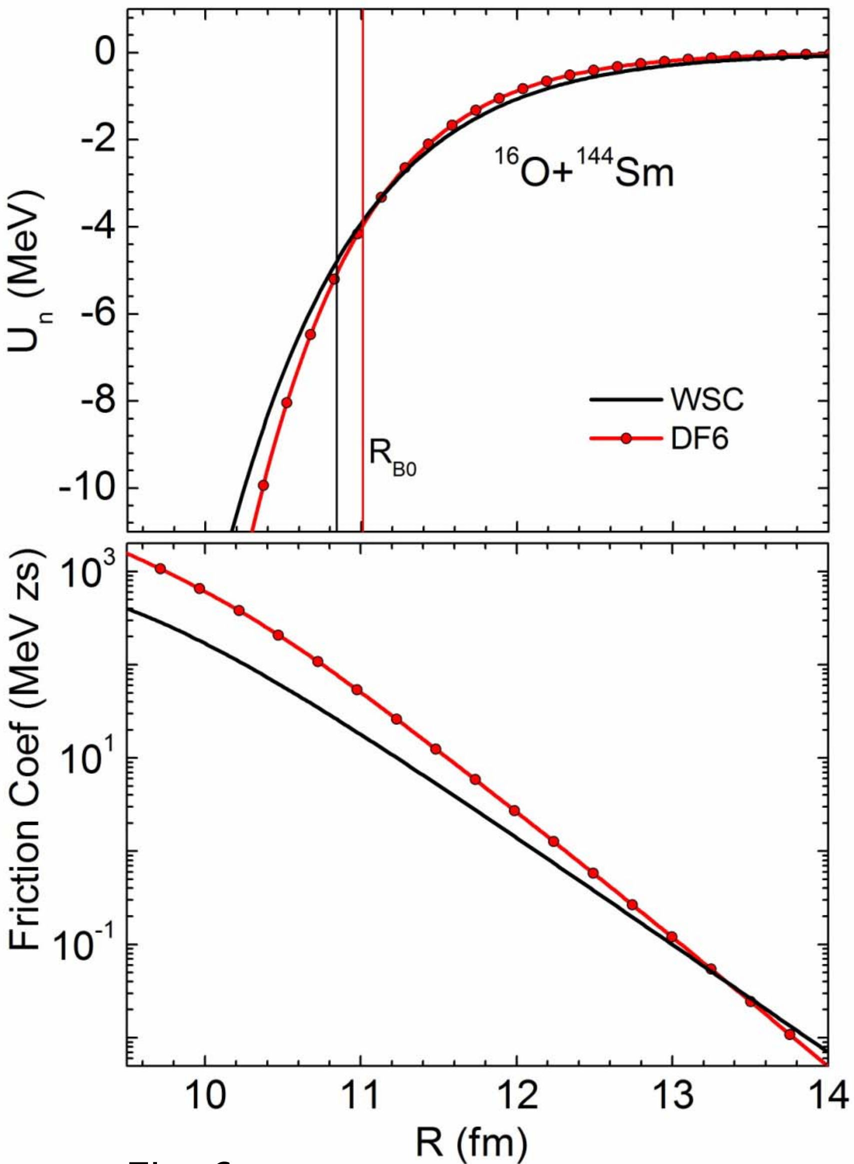

Fig. 6

$$K_R = 2.0\times10^{-2}\ \mathrm{MeV}^{-1}\ \mathrm{zs}$$

$$a_{AT} = 0.510\,\mathrm{fm}$$

$$F_{Dq} = -\frac{p}{m_q}\boxed{K_R\left(\frac{dU_n}{dq}\right)^2} \quad (10)$$

	Gross, Kalinowski (1978)	Fröbrich (1984)	TMSF (2014)
Potential	Single folding	Single folding	Double folding with DD M3Y & finite range exchange term
Forces	1) Conservative 2) instant friction	1) Conservative, 2) instant friction 3) dynamical quadrupole deformations	1) Conservative 2) retarding friction 3) thermal fluctuations
L	continuous	continuous	discrete
Data	~20%	~20%	~1%
Agreement	Figures	Figures	χ^2
Density	Fermi step	Fermi step	Microscopical Hartree-Fock approach

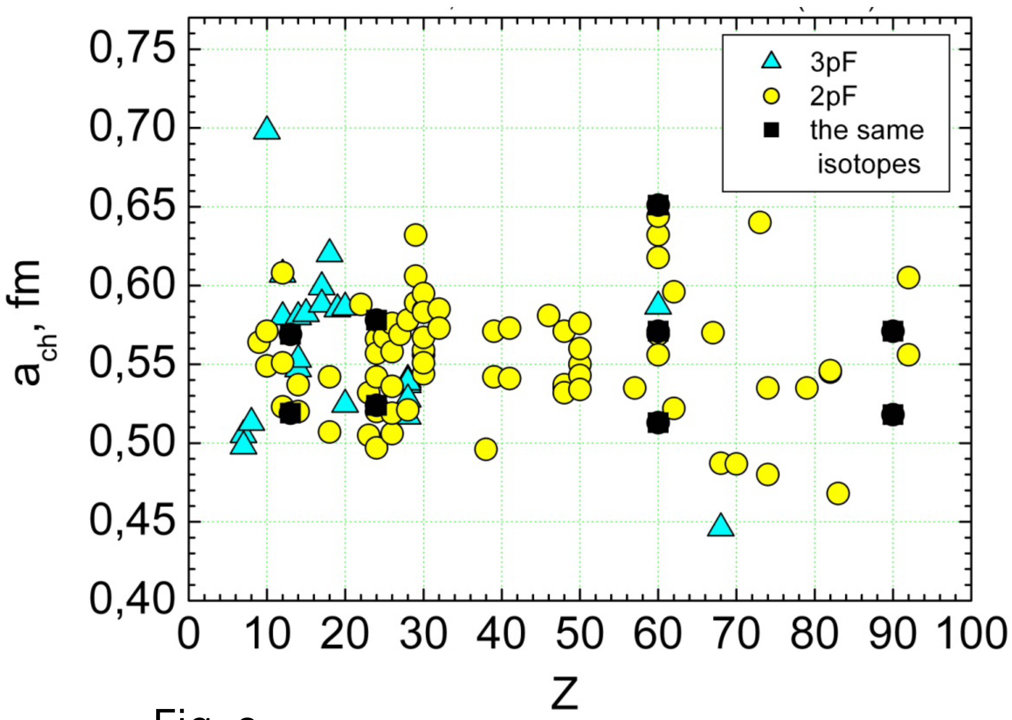

Fig. 9

[7] H. de Vries et al., At. Dat. Nucl. Dat. Tab. 36 (1987) 495

Parameters of the model:

$$
\begin{cases}
K_R : (1 \div 4) \times 10^{-2}\ \mathrm{MeV}^{-1}\mathrm{zs} \\
\tau : (0 \div 1)\ \mathrm{zs} \\
\left.\begin{array}{l} a_{AP} \\ a_{AT} \end{array}\right\} : (0.45 \div 0.60)\ \mathrm{fm} \\
F_{\mathrm{v}}(\rho_{FA}) \\
a_{nP} \neq a_{pP} \\
a_{nT} \neq a_{pT}
\end{cases}
$$

$$R_{PT} = R_P + R_T \qquad (30)$$

$$R = qR_{PT} \qquad (31)$$

$$p_q = pR_{PT} \qquad (32)$$

$$F_q = FR_{PT} \qquad (33)$$

$$m_q = m_n R_{PT}^2 \frac{A_P A_T}{A_P + A_T} \qquad (34)$$

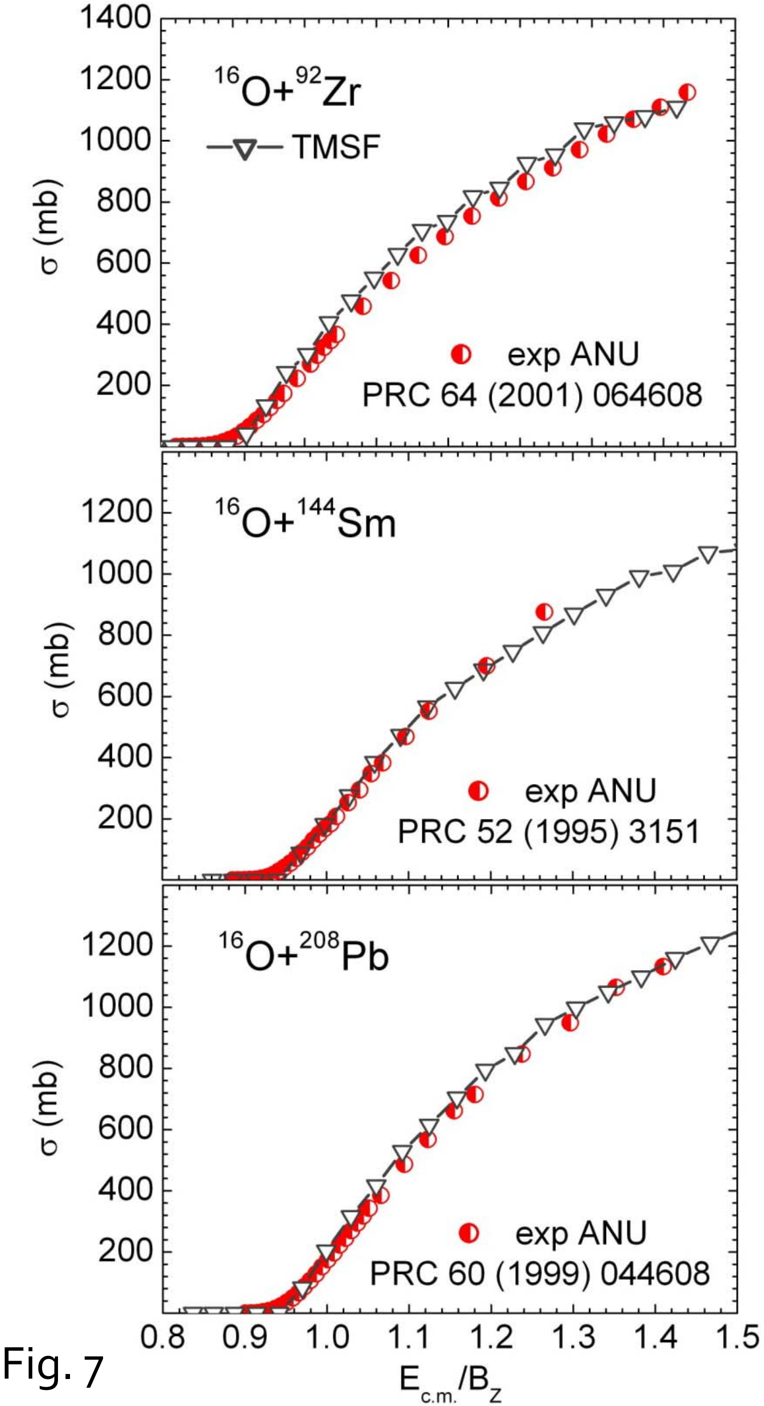

Fig. 7

[6] MC, IG PRC 87 (2013) 014614

(no fluctuations)

TMSF DF2 M3Y

$$K_R = 2.5\times10^{-2}\ \mathrm{MeV}^{-1}\ \mathrm{zs}$$

$$\tau = 0$$

Parameters
of the model:

$$\begin{cases} K_R = 3.5\times10^{-2}\ \mathrm{MeV}^{-1}\mathrm{zs}\,[2]\ \mathrm{or} \\ \qquad 4.0\times10^{-2}\ \mathrm{MeV}^{-1}\mathrm{zs}\,[3] \\ \tau < 1\,\mathrm{zs} \\ \left.\begin{matrix} a_{AP} \\ a_{AT} \end{matrix}\right\} : (0.45 \div 0.60)\ \mathrm{fm} \end{cases}$$

[2] D.H.E. Gross, H. Kalinowski, Phys. Rep. 45 (1978) 175

[3] P. Fröbrich, Phys. Rep. 116 (1984) 337

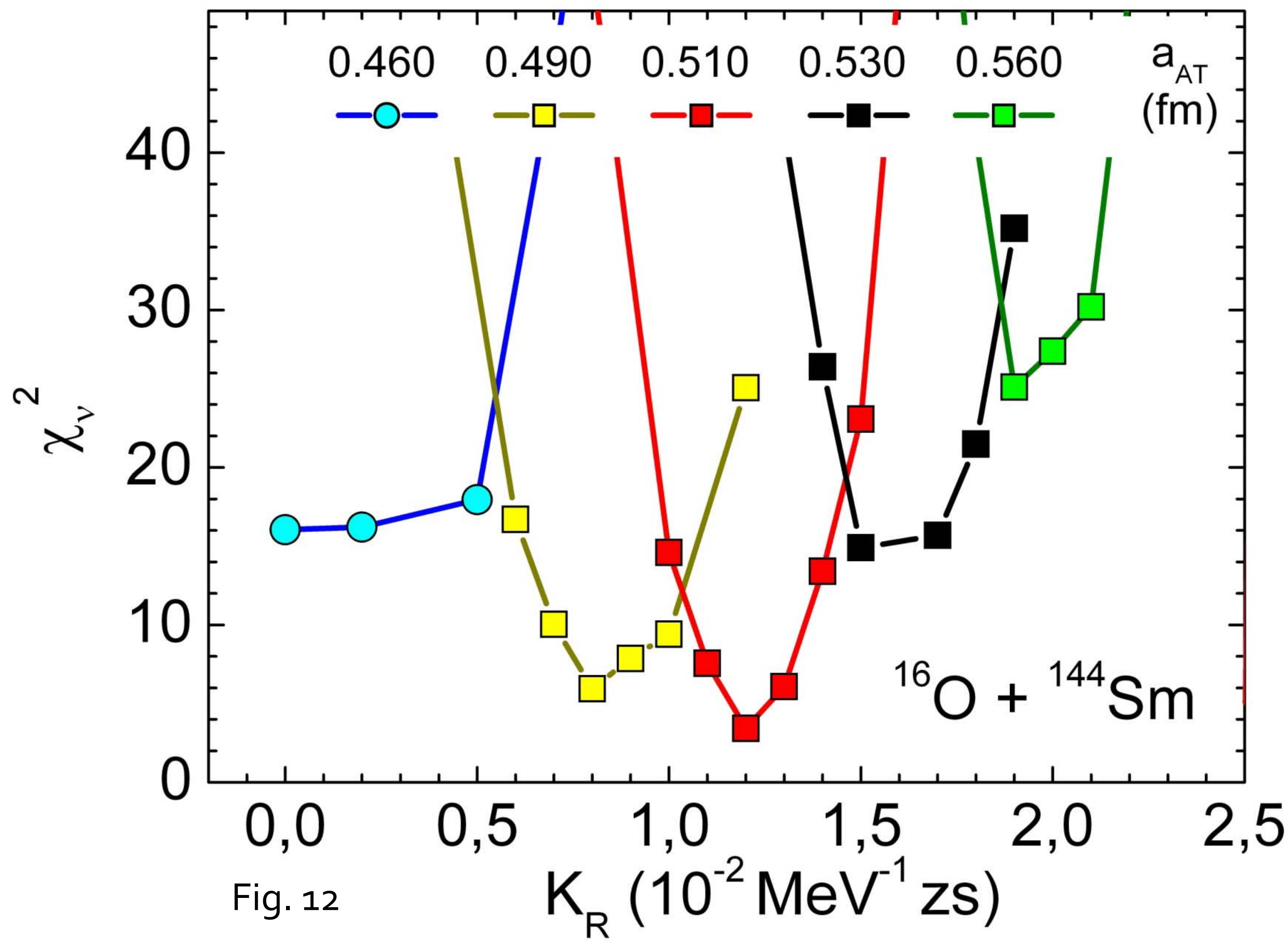

Fig. 12

$$\sigma_{\text{exp}} > 200 \text{ mb}$$
$$\tau = 0$$

[9] ANU data: PRC 52 (1995) 3151

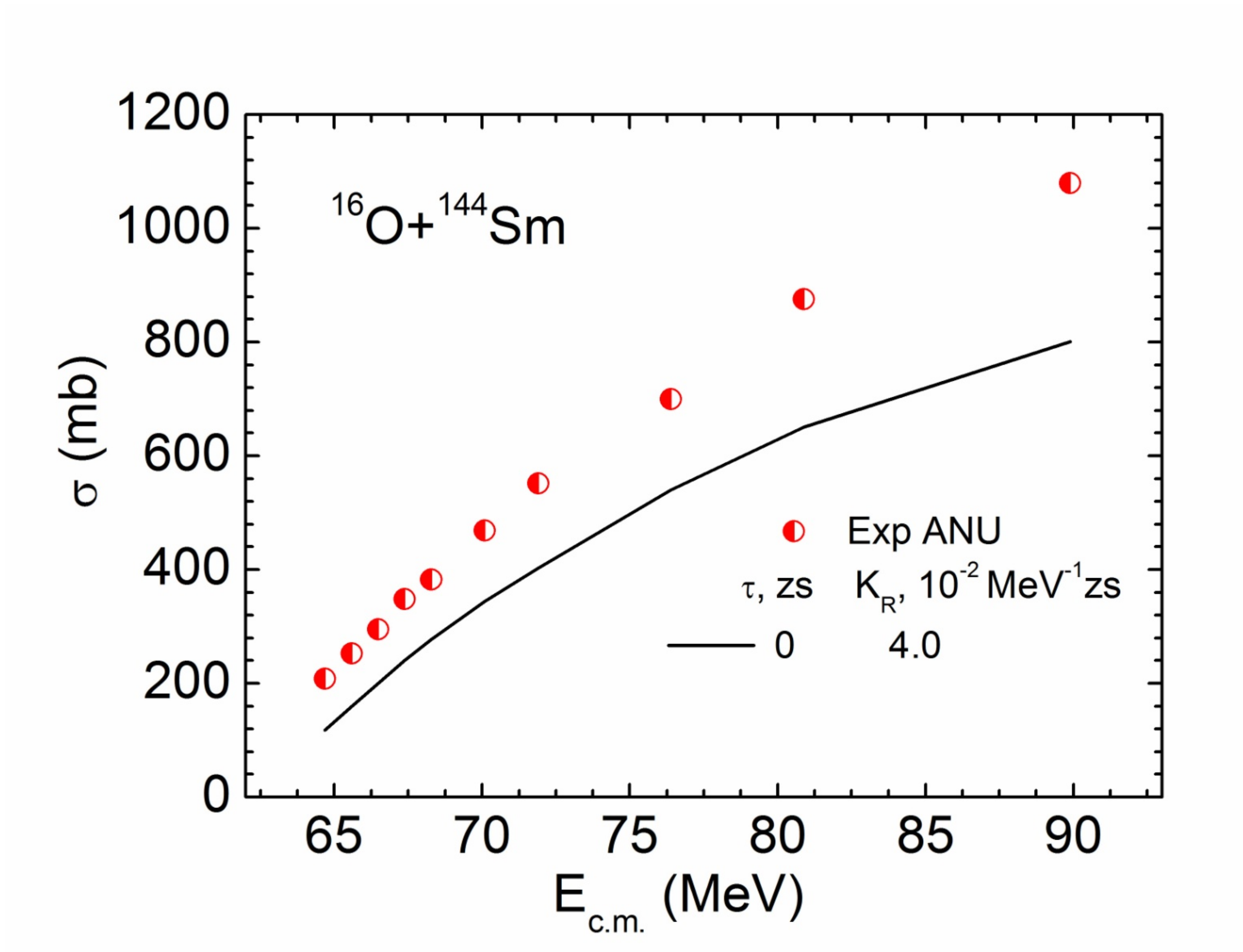
1200
1000
800
600
400
200
0
σ (mb)
^{16}O+^{144}Sm
Exp ANU
τ, zs K$_R$, 10^{-2} MeV^{-1}zs
0 4.0
65
70
75
80
85
90
E$_{c.m.}$ (MeV)

Fig. 13

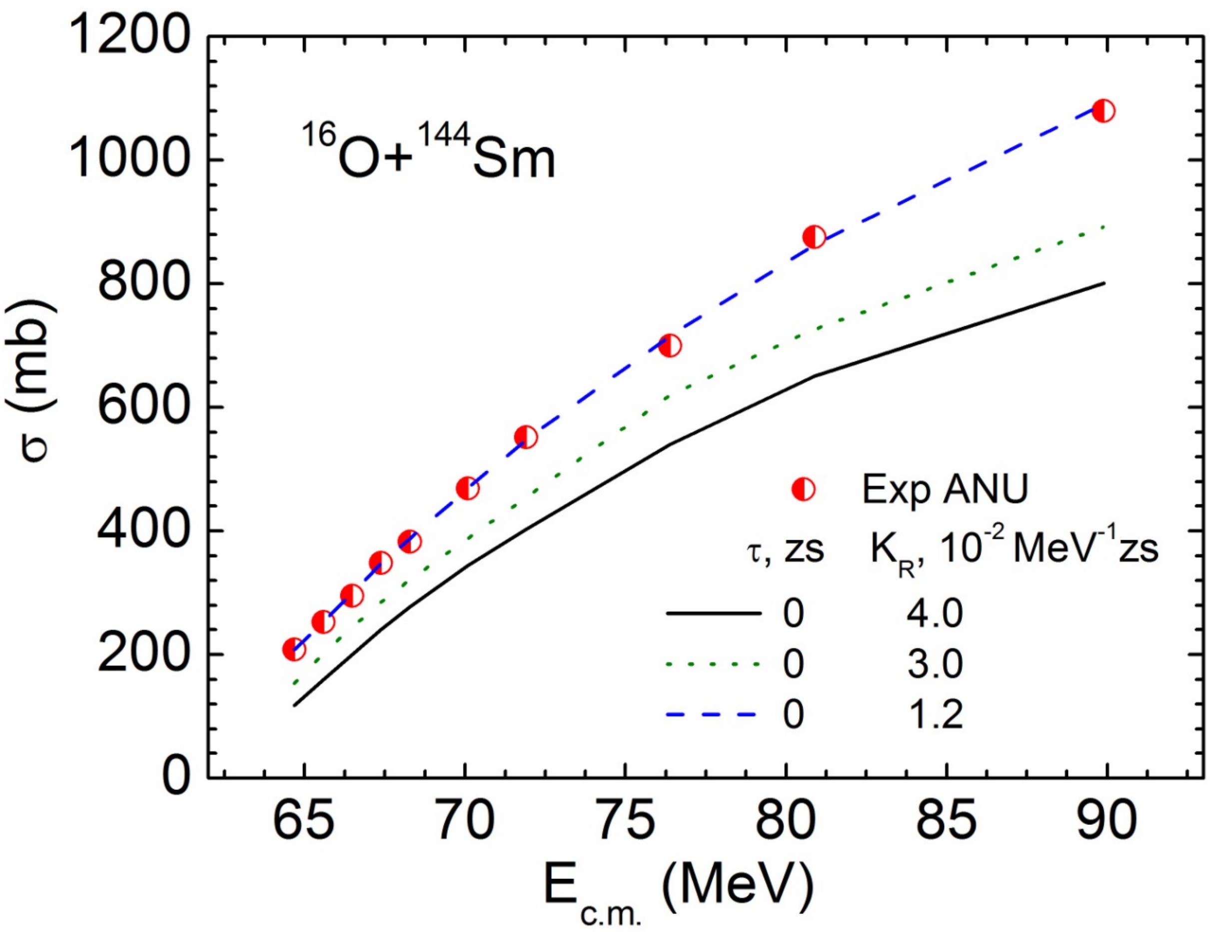

$^{16}O+^{144}Sm$
σ (mb)
1200
1000
800
600
400
200
0
65
70
75
80
85
90
$E_{c.m.}$ (MeV)
Exp ANU
τ, zs K_R, 10^{-2} MeV^{-1}zs
0   4.0
0   3.0
0   1.2

Fig. 13

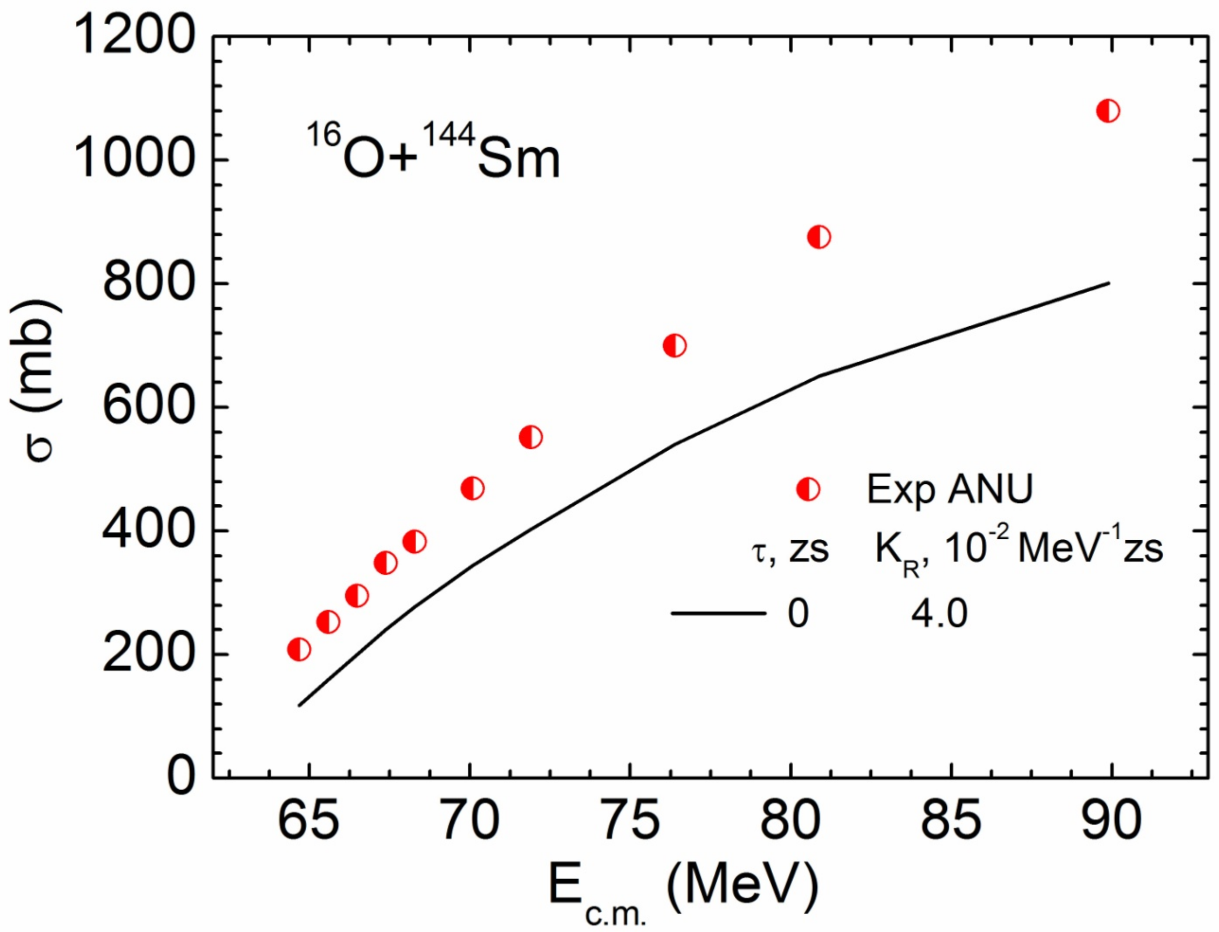

^{16}O+^{144}Sm
Exp ANU
τ, zs K$_R$, 10^{-2} MeV^{-1}zs
0 4.0
σ (mb)
E$_{c.m.}$ (MeV)
0
200
400
600
800
1000
1200
65
70
75
80
85
90

Fig. 13

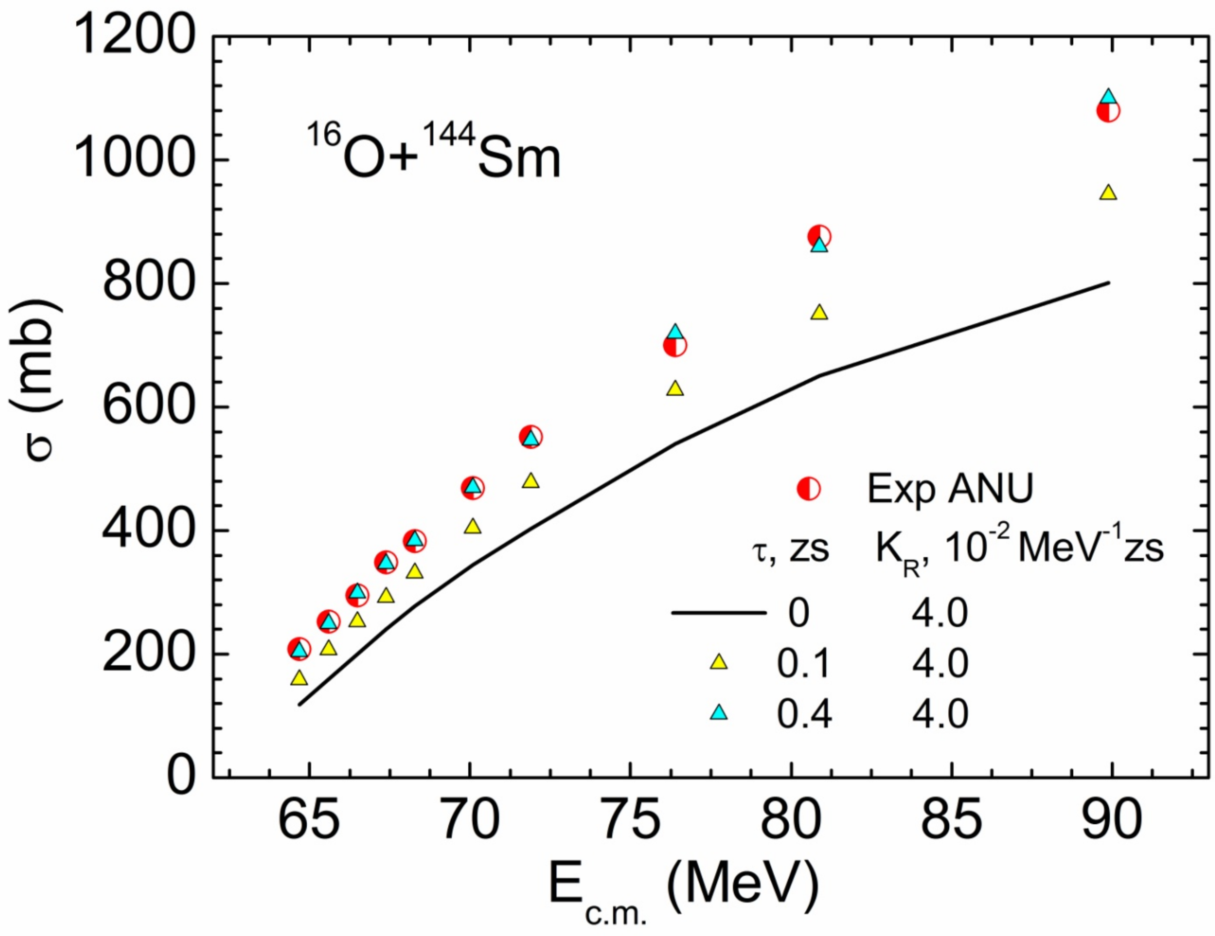

1200
1000
800
600
400
200
0
σ (mb)
16O+144Sm
Exp ANU
τ, zs
K_R, 10^-2 MeV^-1 zs
0 4.0
0.1 4.0
0.4 4.0
65
70
75
80
85
90
E_c.m. (MeV)

Fig. 13

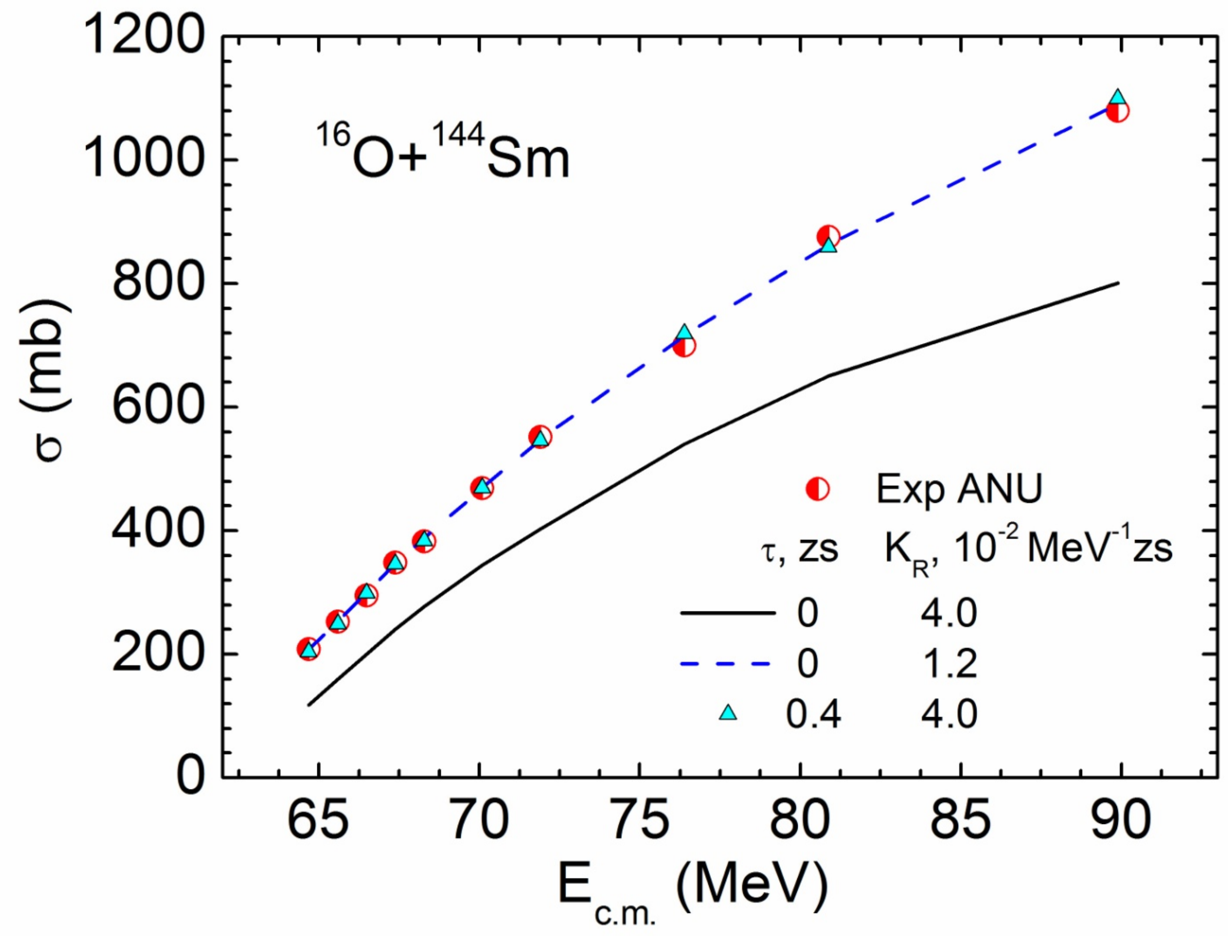

Fig. 13

$$\Phi_{Dq} = -\int_0^t F_{Dq}(s)\Gamma(t-s)\,ds \quad (9)$$

$$^{16}\mathrm{O} + {}^{144}\mathrm{Sm}$$

ANU data: J.R. Leigh et al., PRC 52 (1995) 3151

ANU analysis: PRC 70 (2004) 024605	This work (2013)
SBPM	TMSF
Woods-Saxon potential	Double folding (M3Y DD6)
$a_{WS} = 0.75\ \mathrm{fm}$	$a_{DF} = 0.68\ \mathrm{fm}$
$\chi_\nu^2 = 6.3$	$\chi_\nu^2 = 3.4$

$$\lambda = \frac{2\pi\hbar}{p} \qquad (35)$$

$$\hbar = 0.6588\ MeV \cdot zs \qquad (36)$$

$$^{16}\mathrm{O} + {}^{92}\mathrm{Zr}$$

$$p_R \approx 4\ MeV \cdot zs \cdot fm^{-1} \qquad (37)$$

$$\lambda = 1.0\ fm \qquad (38)$$

$$R_T = 4.9\ fm \qquad (39)$$

$$R_T > \lambda \qquad (40)$$

The Need for Precise Experimental Above-Barrier Cross Sections:

Symmetric reactions:

$^{12}C + {}^{12}C$

$^{16}O + {}^{16}O$

$^{31}P + {}^{31}P$

$^{32,34,36,38}S + S$

$^{37}Cl + {}^{37}Cl$

$^{40,48}Ca + {}^{40,48}Ca$

$^{58}Ni + {}^{58}Ni$

Another above-barrier cross sections:

$^{12}C + {}^{28}Si, {}^{58}Ni, Ca, {}^{89}Y$

$^{28}Si + {}^{58}Ni, {}^{92}Zr, {}^{144}Sm, {}^{208}Pb$

$^{31}P + \text{spherical nuclei}$

$^{32}S + {}^{28}Si, {}^{40}Ca, {}^{58}Ni, {}^{92}Zr, {}^{144}Sm$

$^{37}Cl + \text{spherical nuclei}$

$^{40}Ar + {}^{112,120}Sn, {}^{144}Sm, {}^{208}Pb, {}^{209}Bi$

Double folding model

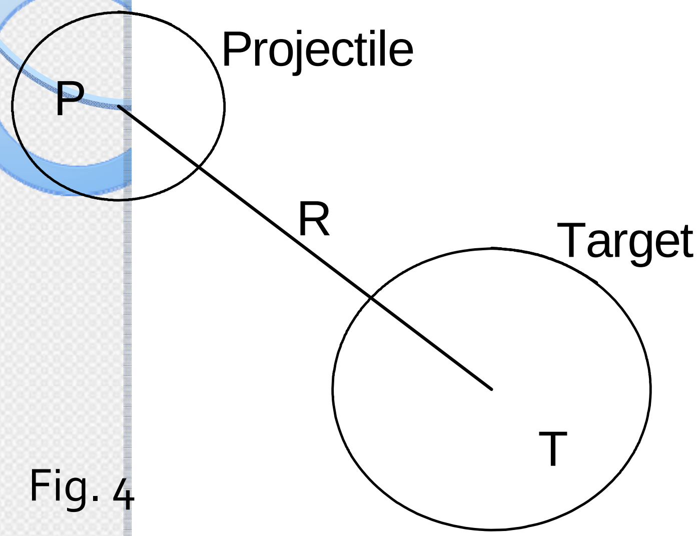

Fig. 4

$$U_{PT}(R) = U_n(R) + U_C(R) \qquad (41)$$

$$U_n(R) \to U_{nD}(R), \quad U_{nE}(R)$$

Direct part of the nuclear term:

$$U_{nD}(R) = g\int d\vec{r}_P \int d\vec{r}_T \rho_{PA}(\vec{r}_P) F(\rho_{FA}) \mathrm{v}_D(\vec{s}) \rho_{TA}(\vec{r}_T) \qquad (42)$$

Exchange part of the nuclear term:

$$U_{nE}(R) = g\int d\vec{r}_P \int d\vec{r}_T \rho_{PA}(\vec{r}_P; \vec{r}_P + \vec{s}) \times$$
$$\times F(\rho_{FA}) \mathrm{v}_E(\vec{s}) \rho_{TA}(\vec{r}_T; \vec{r}_T - \vec{s}) \exp\left(i\vec{k}_{rel}\,\vec{s}/A_{red}\right) \qquad (43)$$

Density dependence:

$$F(\rho_{FA}) = C_F \{1 + \alpha_F \exp(-\beta_F \rho_{FA}) - \gamma_F \rho_{FA}\} \quad (44)$$

$$\rho_{FA} = \rho_{PA}(\vec{r}_P + \vec{s}/2) + \rho_{TA}(\vec{r}_T - \vec{s}/2) \quad (45)$$

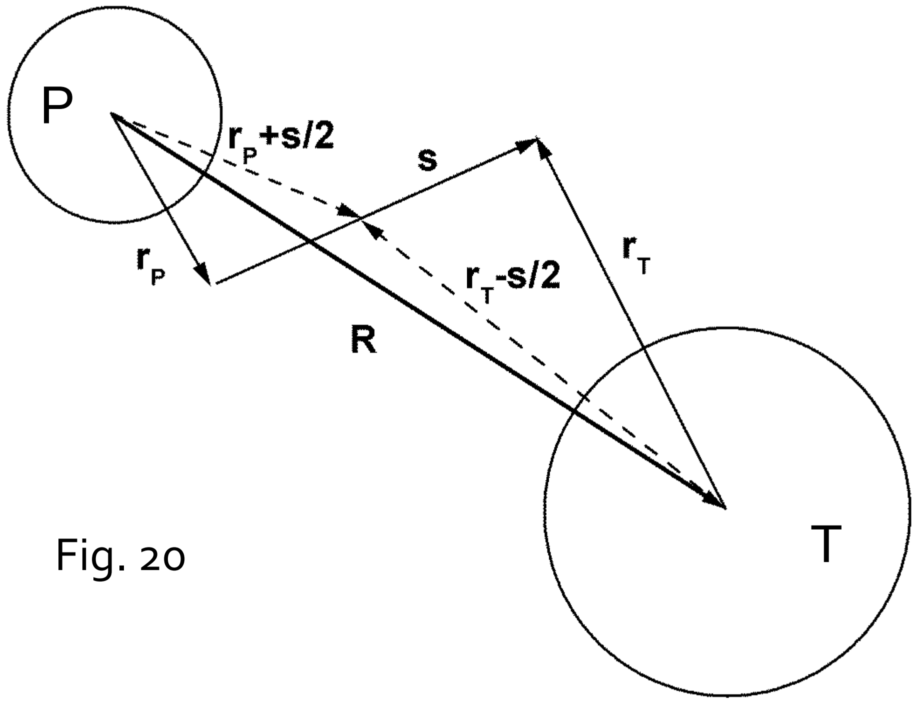

Fig. 20

Density dependence:

$$F(\rho_{FA}) = C_F \{1 + \alpha_F \exp(-\beta_F \rho_{FA}) - \gamma_F \rho_{FA}\} \quad (44)$$

DD label	Interaction	C	α	$\beta(\mathrm{fm}^{-3})$	$\gamma(\mathrm{fm}^{-3})$
0	D independent	1	0.0	0.0	0.0
1	DDM3Y1	0.2963	3.7231	3.7384	0.0
2	CDM3Y1	0.3429	3.0232	3.5512	0.5
3	CDM3Y2	0.3346	3.0357	3.0685	1.0
4	CDM3Y3	0.2985	3.4528	2.6388	1.5
5	CDM3Y4	0.3052	3.2998	2.3180	2.0
6	CDM3Y5	0.2728	3.7367	1.8294	3.0
7	CDM3Y6	0.2658	3.8033	1.4099	4.0
8	BDM3Y1	1.2521	0.0	0.0	1.7452

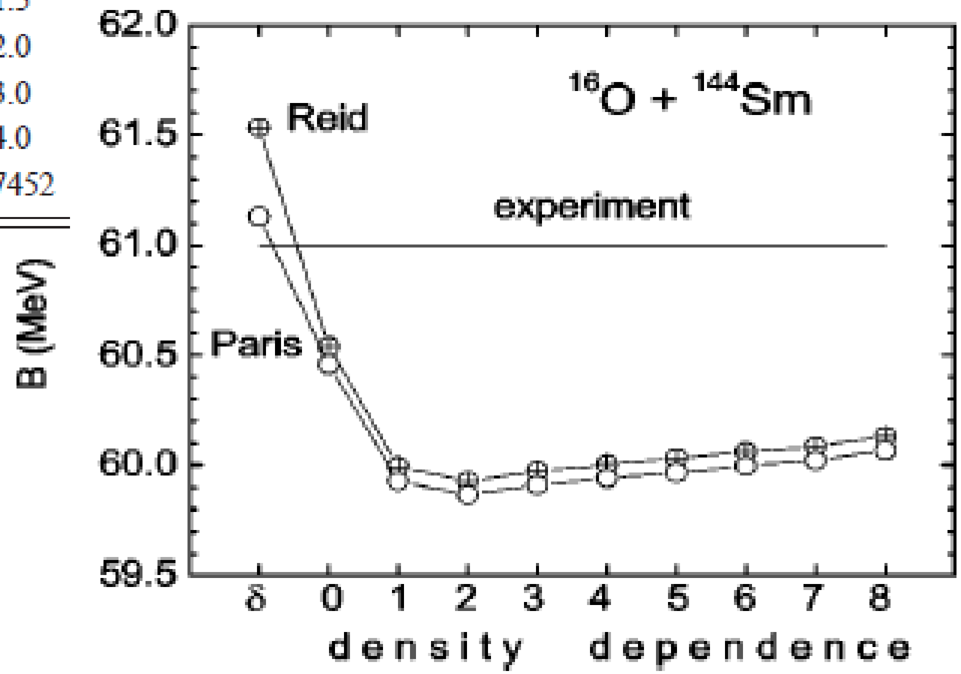

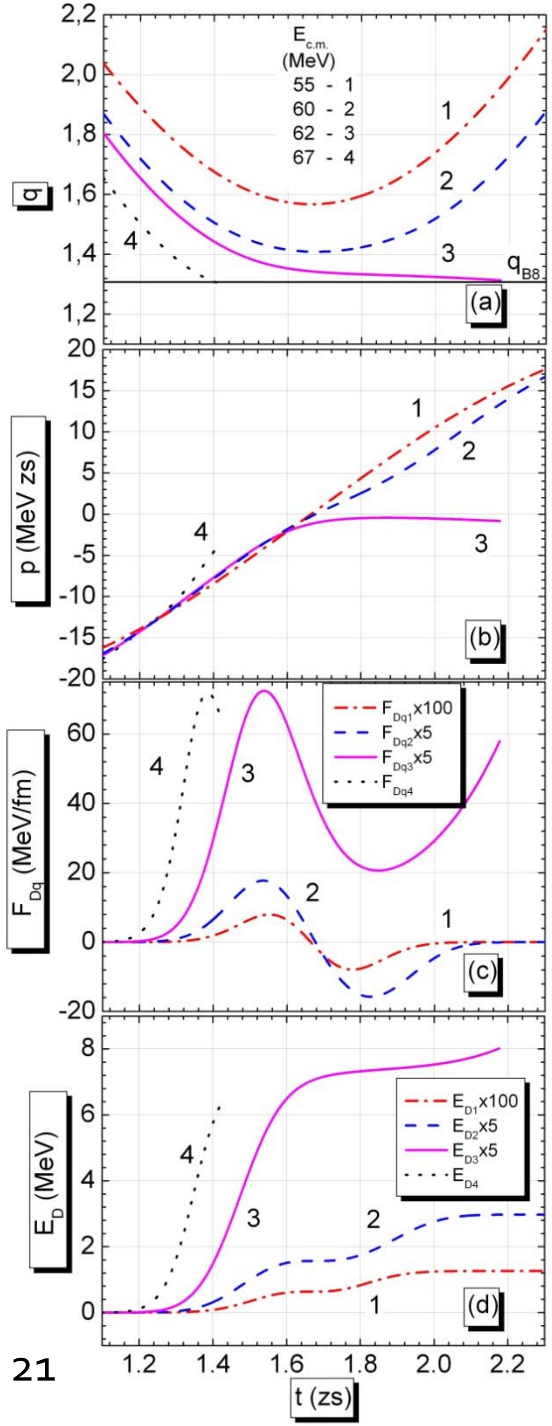

E c.m. (MeV)
55 - 1
60 - 2
62 - 3
67 - 4
q
q B8
(a)
p (MeV zs)
(b)
F Dq (MeV/fm)
F Dq1 x100
F Dq2 x5
F Dq3 x5
F Dq4
(c)
E D (MeV)
E D1 x100
E D2 x5
E D3 x5
E D4
(d)
t (zs)

Fig. 21

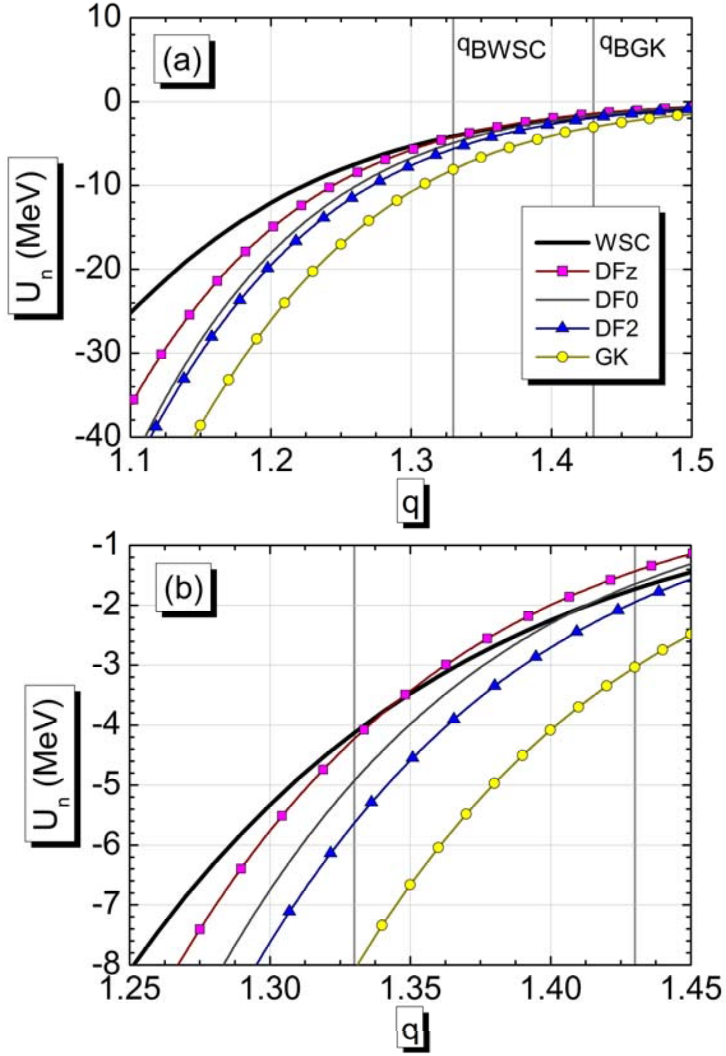

(a)
q BWSC
q BGK
U n (MeV)
WSC
DFz
DF0
DF2
GK
q
(b)
U n (MeV)
q

Fig. 22

$$p_{0L} = \sqrt{2m_q\left[E_{c.m.} - U_C\left(q_0\right) - U_n\left(q_0\right) - U_{cen}\left(q_0, L\right)\right]} \qquad (46)$$

$$U_n\left(R\right) = \ln\left\{1 + \exp\left(-\frac{\Delta R}{a_{GK}}\right)\right\}\left[A_{0GK} + A_{1GK}\Delta R + A_{2GK}\Delta R^2\right] \qquad (47)$$

$$\Delta R = R - r_{GK}\left(A_P^{1/3} + A_T^{1/3}\right) \qquad (48)$$

$$\left.\begin{array}{lll} r_{0GK} = 1.30 \text{ fm} & a_{GK} = 0.61 \text{ fm} & \\ A_{0GK} = 33 \text{ MeV} & A_{1GK} = 2 \text{ MeV} & A_{2GK} = 3 \text{ MeV} \end{array}\right\} \qquad (49)$$

TABLE II. Parameters of the potentials for the system $^{16}O + {}^{92}Zr$ displayed in Figs. 2-10, 12 and 13

Potential	q_{B11}	R_{B11}, fm	U_{B11}, MeV	Parameters of the potential
WSC	1.330	10.00	41.94	$a_{WS} = 0.841 fm,\ r_{WS} = 1.046 fm,\ V_{WS} = -100.0 MeV$ [1]
DFz	1.360	10.23	41.96	$A_0 = 21.5$ MeV, $A_1 = 3.2$ MeV, $A_2 = 0.0$ MeV, $r_0 = 1.28$ fm, $a = 0.60$ fm
DF0	1.377	10.36	41.51	$A_0 = 21.0$ MeV, $A_1 = 3.4$ MeV, $A_2 = 0.2$ MeV, $r_0 = 1.30$ fm, $a = 0.58$ fm
DF2	1.392	10.47	41.06	$A_0 = 20.5$ MeV, $A_1 = 4.8$ MeV, $A_2 = 4.4$ MeV, $r_0 = 1.32$ fm, $a = 0.50$ fm
GK	1.430	10.76	39.81	as in Eq.(10)
DFz, DF0, DF2				$R_P = 2.608 fm,\ a_P = 0.465 fm,\ R_T = 4.913 fm,\ a_T = 0.533 fm$ [19]

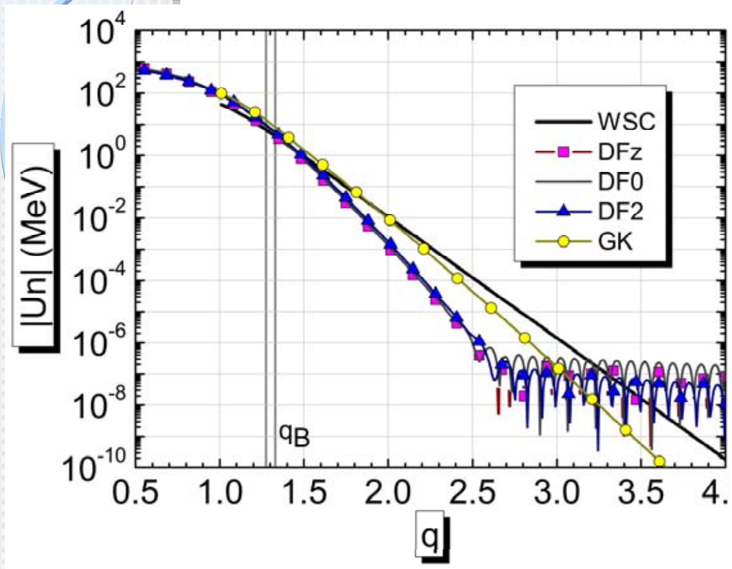

Fig. 23

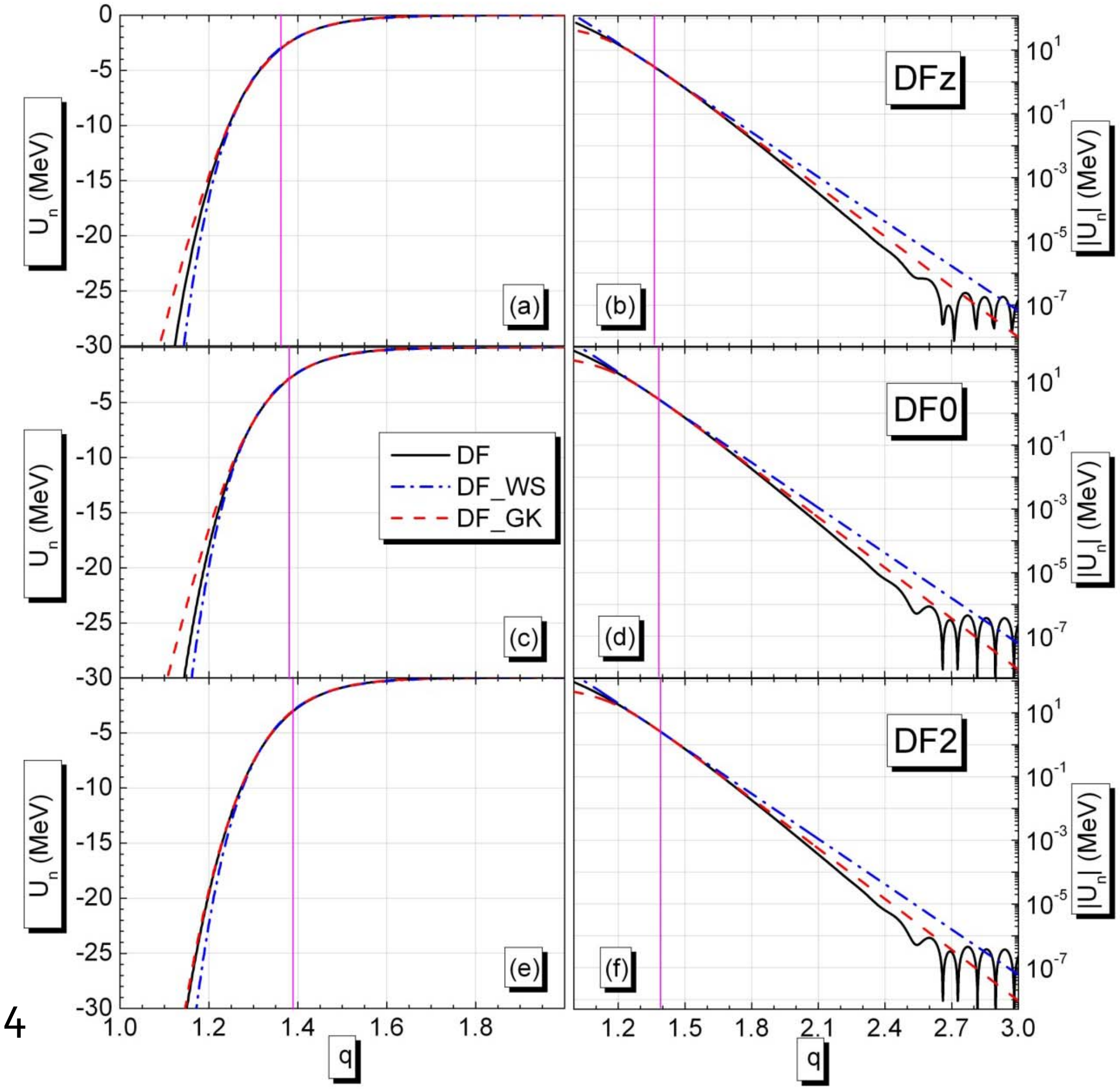

Fig. 24

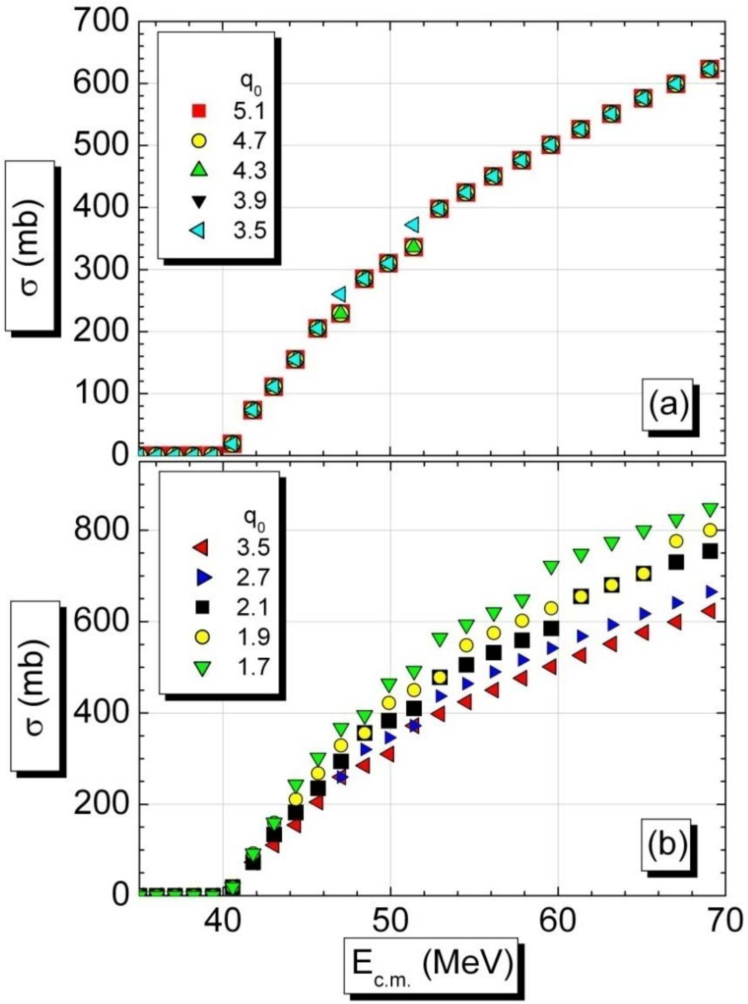

q0
5.1
4.7
4.3
3.9
3.5
q0
3.5
2.7
2.1
1.9
1.7
(a)
(b)
σ (mb)
σ (mb)
Ec.m. (MeV)

Fig. 25

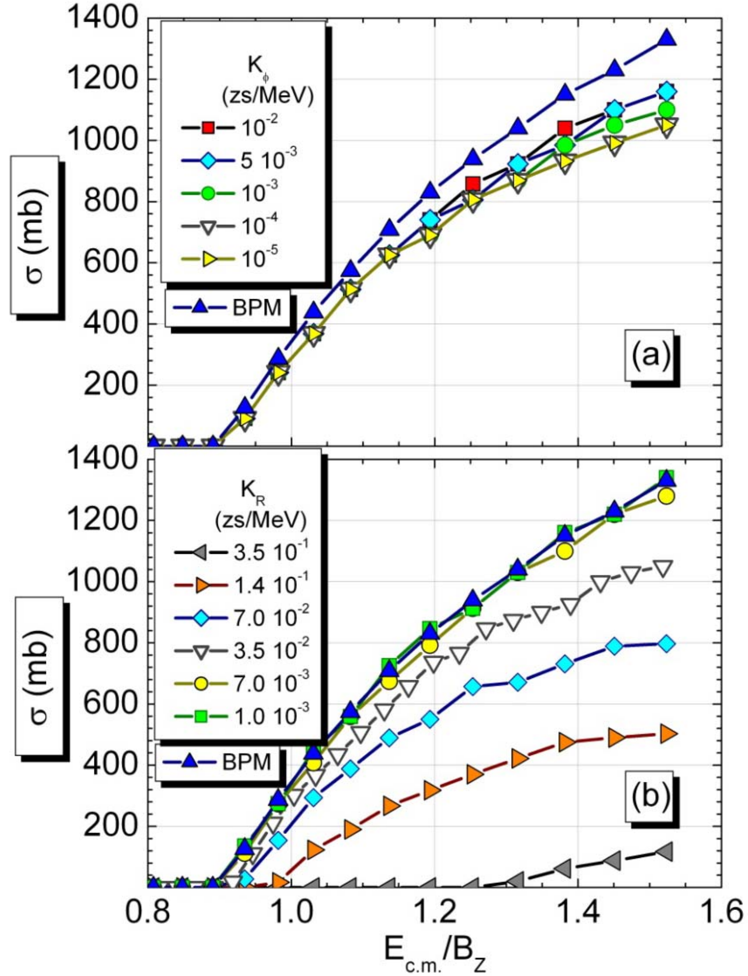

Kϕ
(zs/MeV)
10-2
5 10-3
10-3
10-4
10-5
BPM
KR
(zs/MeV)
3.5 10-1
1.4 10-1
7.0 10-2
3.5 10-2
7.0 10-3
1.0 10-3
BPM
(a)
(b)
σ (mb)
σ (mb)
Ec.m./BZ

Fig. 26

$$\theta = \sqrt{E_{DP(T)}\left(a_1 A_{P(T)} + a_2 A_{P(T)}^{2/3}\right)^{-1}} \qquad (50)$$

$$a_1 = 0.073 \text{ MeV}^{-1} \qquad a_2 = 0.095 \text{ MeV}^{-1}$$

[20] A. V. Ignatyuk et al., Yad. Fiz. 21 (1975) 1185

$$E_D = E_{DP} + E_{DT} = E_{cm} - \frac{p_q^2}{2m_q} - \frac{\hbar^2 L^2}{2m_q q^2} - U_{tot}$$

$$\mathrm{v}_D(s) = \sum_{i=1}^{3} G_{Di}[\exp(-s/r_{\mathrm{v}i})]/(s/r_{\mathrm{v}i}) \qquad (51)$$

$$\mathrm{v}_{Ef}(s) = \sum_{i=1}^{3} G_{Efi}[\exp(-s/r_{\mathrm{v}i})]/(s/r_{\mathrm{v}i}) \qquad (52)$$

$$\mathrm{v}_{E\delta}(\vec{s}) = G_{E\delta}\,\delta(\vec{s}) \qquad (53)$$

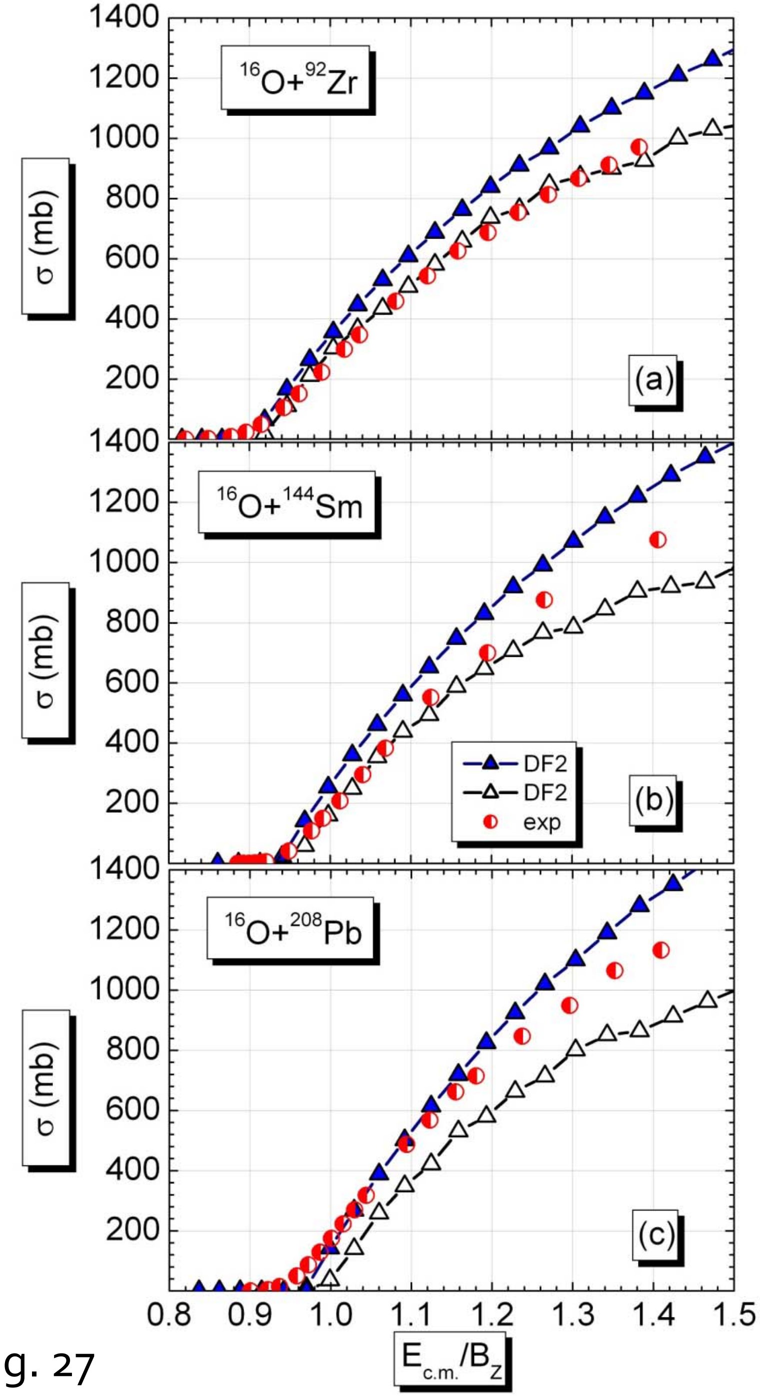

Fig. 27

← SBPM DF2 M3Y

← TMSF DF2 M3Y

$$K_R = 3.5\times10^{-2}\, zs\, MeV^{-1}$$

[6] J.O. Newton et al., PRC 64 (2001) 064608

[7] J.R. Leigh et al., PRC 52 (1995) 3151

[8] C.R. Morton et al., PRC 60 (1999) 044608

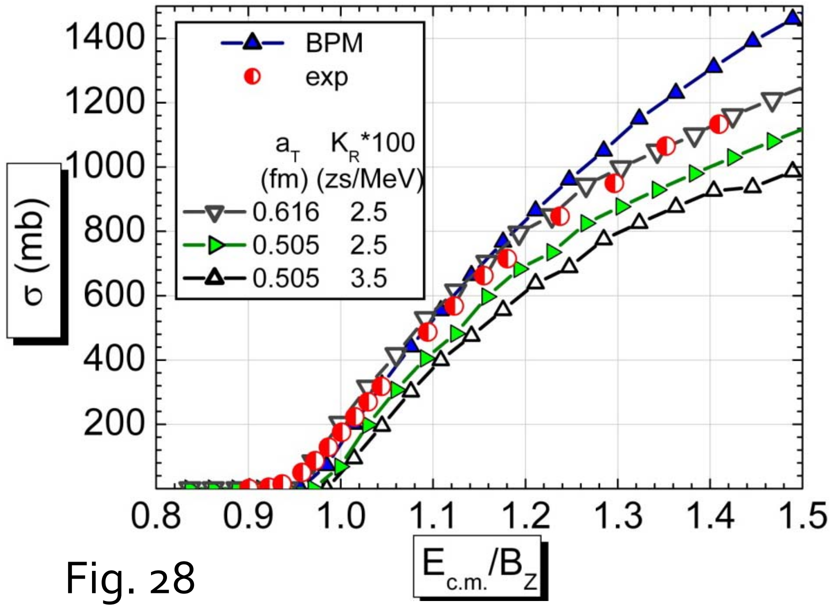

Fig. 28

$$\sigma = \frac{\pi\hbar^2}{2m_R E_{c.m.}} \sum_{L=0}^{L_{\max}} (2L+1) T_L \qquad (1)$$

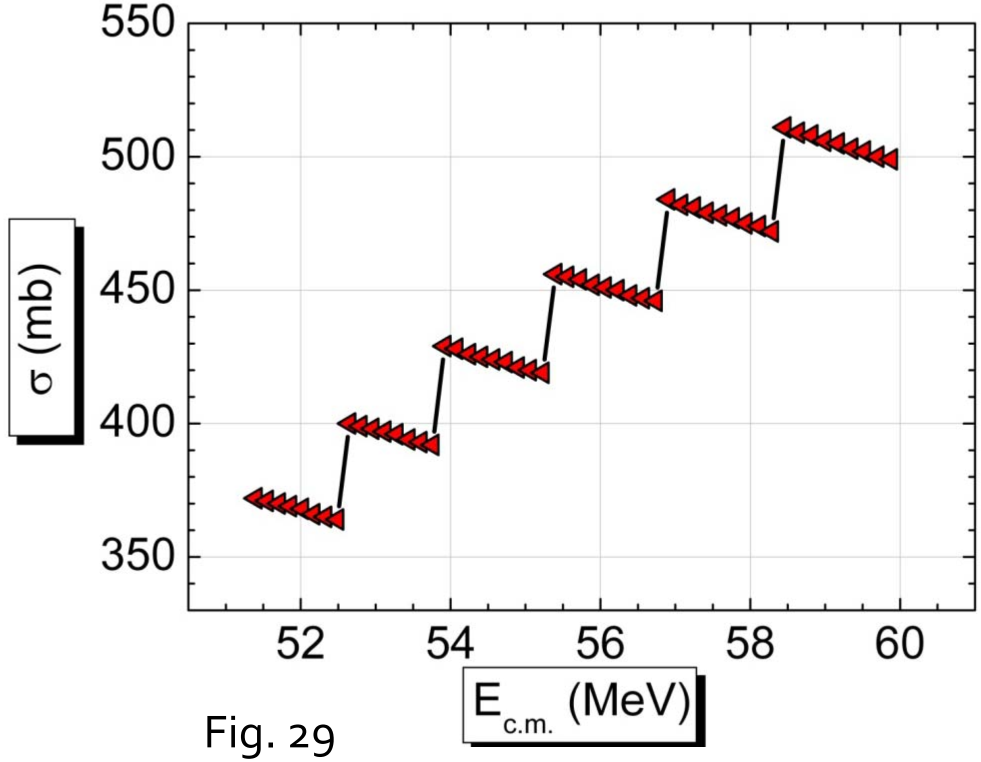

Fig. 29

SYSTEMATIC COMPARISON OF HEAVY-ION FUSION BARRIERS CALCULATED WITHIN THE FRAMEWORK OF THE DOUBLE FOLDING MODEL USING TWO VERSIONS OF NUCLEON-NUCLEON INTERACTION

Gontchar I.I.[1], Chushnyakova M.V.[2,3]
[1] *Omsk State Transport University, Omsk, Russia;*
[2] *Omsk State Technical University, Omsk, Russia;*
[3] *Tomsk Polytechnic University, Tomsk, Russia*
E-mail: vigichar@hotmail.com

It was shown in Refs. [1, 2] that the high energy parts of the heavy ion fusion excitation functions can be successfully reproduced within the framework of the double folding approach. The major ingredients of this approach are the nuclear densities and the effective nucleon-nucleon interaction [3]. In [1, 2] the well-known M3Y *NN* forces [4, 5] were used. However sometimes in the literature the Migdal *NN* forces [6] are used to calculate the nucleus-nucleus potential [7, 8]. The question is to what extent the fusion barrier heights are different when calculating interaction potentials within the double folding approach with two options of the nucleon-nucleon interaction: the M3Y and the Migdal ones.

In the present work we address this question performing systematic calculations of the fusion barrier height for zero angular momentum, U_{B0}. In our calculations the nuclear densities came from the Hartree-Fock approach with the SKX coefficient set [9, 10]. The charge densities obtained within these calculations are shown to be in good agreement with the experimental data [11, 12]. The values of U_{B0} are calculated in the wide range of the value of the parameter $B_Z = Z_P Z_T / \left(A_P^{1/3} + A_T^{1/3} \right)$: it varies from 10 MeV up to 150 MeV. Only spherical nuclei from ^{12}C up to ^{208}Pb are considered.

Our calculations make it possible to draw definite conclusions about the applicability of the Migdal *NN* forces for describing the nucleus-nucleus collision.

1. I.I.Gontchar *et al*. // Phys. Rev. C. 2014. V.89. 034601.
2. M.V.Chushnyakova *et al*. // Phys. Rev. C. 2014. V.90. 017603.
3. Dao T.Khoa *et al*. // Phys. Rev. C. 1997. V.56. P.954.
4. G.Bertsch *et al*. // Nucl. Phys. A. 1977. V.284. P.399.
5. N.Anantaraman *et al*. // Nucl. Phys. A. 1983. V.398. P.269.
6. A.B.Migdal. Theory of Finite Fermi Systems and Application to Atomic Nuclei. New York: Interscience Publishers. 1967. P.319.
7. N.V.Antonenko *et al*. // Phys. Rev. C. 1994. V.50. P.2063.
8. V.I.Zagrebaev *et al*. // Phys. Elem. Part. At. Nucl. 2007. V.38. P.469.
9. B.A.Brown // Phys. Rev. C. 1998. V.58. P.220.
10. R.Bhattacharya // Nucl. Phys. A. 2013. V.913. P.1.
11. H.de Vries *et al*. // At. Dat. Nucl. Dat. Tables. 1987. V.36. P.495.
12. I.Angeli // At. Dat. Nucl. Dat. Tables. 2004. V.87. P.185.